POLAR CODED COMMUNICATION SYSTEM DESIGN

FATİH GENÇ

SEPTEMBER 2021

ÇANKAYA UNIVERSITY

GRADUATE SCHOOL OF NATURAL AND APPLIED SCIENCES

DEPARTMENT OF ELECTRONIC AND COMMUNICATION ENGINEERING

PH.D THESIS IN

ELECTRONIC AND COMMUNICATION ENGINEERING

POLAR CODED COMMUNICATION SYSTEM DESIGN

FATİH GENÇ

SEPTEMBER 2021

ABSTRACT

POLAR CODED COMMUNICATION SYSTEM DESIGN

GENÇ, Fatih

PhD in Electronic and Communication Engineering

Supervisor: Assoc. Prof. Dr. Orhan GAZİ

September 2021, 77 pages

In 2008, polar codes, which are the only channel codes whose performance are mathematically proven, are introduced by Arıkan. The introduction of polar codes was a milestone in coding society. The implementation of polar codes at high speeds is of critical importance, especially in communication systems such as 5G where high speed and parallel processing ICs such as FPGA are employed. In FPGA technology, it is of critical importance how much space the algorithm occupies in the integrated chip. The area occupied by the algorithm is directly proportional to the energy use of the FPGA and the delay of the process. In this thesis, we propose a polar encoding method that occupies less hardware implementation space. It is seen that with the innovative polar encoding scheme, considering the implementation area used, a noticeable advantage for FPGA implementations is achieved.

We also analyse the performance of polar codes with pilot-based channel estimation and equalization methods. By using the frozen bits of the polar codes, the pulse and frequency responses of the communication channels can be estimated. Among the estimation and equalizer methods, least squares and minimum mean square (MMSE) methods are used. The employment of frozen bits provides an advantage in increasing both the processing speed and the data rate in the receiver at the same time. This is because there is no need

for different packet structures and operations in the communication protocol for channel estimation and equalization.

Keywords: Pole codes, error correction, channel estimation, channel matching, FPGA, code optimization, successive cancelation, VHDL implementation.

ÖZ

POLAR KODLU HABERLEŞME SİSTEMİ TASARIMI

GENÇ, Fatih
Doktora, Elektronik ve Haberleşme Mühendisliği

Tez Yöneticisi: Doç. Dr. Orhan GAZİ
Eylül 2021, 77 Sayfa

2008 yılında performansı matematiksel olarak kanıtlanmış tek kanal kodları olan polar kodlar Arıkan tarafından tanıtılmıştır. Kutup kodlarının tanıtılması, kodlama toplumunda bir kilometre taşıydı. Polar kodların yüksek hızlarda uygulanması, özellikle FPGA gibi yüksek hızlı ve paralel işlem IC'lerinin kullanıldığı 5G gibi iletişim sistemlerinde kritik öneme sahiptir. FPGA teknolojisinde algoritmanın entegre çipte ne kadar yer kapladığı kritik öneme sahiptir. Algoritmanın kapladığı alan, FPGA'nın enerji kullanımı ve işlemin gecikmesi ile doğru orantılıdır. Bu tezde, daha az donanım uygulama alanı kaplayan bir kutupsal kodlama yöntemi öneriyoruz. Yenilikçi polar kodlama şeması ile kullanılan uygulama alanı dikkate alındığında FPGA uygulamaları için gözle görülür bir avantaj sağlandığı görülmektedir.

Bu tezde ayrıca pilot tabanlı kanal tahmini ve eşitleme yöntemleri ile polar kodların performansını da analiz ediyoruz. Kutupsal kodların donmuş bitlerini kullanarak, iletişim kanallarının darbe ve frekans yanıtları tahmin edilebilir. Tahmin ve eşitleyici yöntemlerden en küçük kareler ve minimum ortalama kareler (MMSE) yöntemleri kullanılmaktadır. Dondurulmuş bitlerin kullanılması, alıcıdaki hem işlem hızının hem de veri hızının aynı anda arttırılmasında bir avantaj sağlar. Bunun nedeni, kanal tahmini ve eşitleme için iletişim protokolünde farklı paket yapılarına ve işlemlere gerek olmamasıdır.

Anahtar Kelimeler: Kutup kodları, hata düzeltme, kanal kestirimi, kanal eşleştirme, FPGA, kod optimizasyonu, ardışık giderim algoritması.

ACKNOWLEDGEMENT

The author would like to express sincere gratitude to his supervisor Assoc. Prof. Dr. Orhan GAZİ for their encouragement, guidance, valuable support and patience throughout this study.

The author is also indebted to his parents, Lecturer Leman Genç, Dr. Ramazan Genç, Sultan Uzuner and her sister Assoc. Prof. Dr. Fatma Deniz Uzuner for enlightening me with their, inspiration, understanding, endless love, guidance and wisdom through his entire life.

TABLE OF CONTENTS

LIST OF TABLES

LIST OF FIGURES

LIST OF ABBREVIATIONS

ABA : Average Based Assumption

ASIC : Application Specific Integrated Circuit

AWGN : Additive White Gaussian Noise

BCH : Bose–Chaudhuri–Hocquenghem

B-DMC : Binary-Discrete Memoryless Channel

BEC : Binary Erasure Channel

BER : Bit Error Rate

BLER : Block Error Rate

BMS : Binary input Memoryless Symmetric

BP : Belief Propagation

BPL : Belief Propagation List

BPSK : Binary Phase Shift Keying

BRAM : Block RAM

BSC : Binary Symmetric Channel

CMOS : Complementary Metal Oxide Semiconductor

CNT : Carbon Nanotube

CORR : Correlation based Decision

CRC : Cyclic Redundancy Check

CTC : Convolutional Turbo Code

DE : Density Evolution

DMC : Discrete Memoryless Channel

EEG : Electroencephalogram

eMBB : Enhanced Mobile Broadband

EMG : Electromyography

EXIT : Extrinsic Information Transfer Chart

FEC : Forward Error Correction

FET : Field-Effect Transistor

FG : Factor Graph

5G : Fifth Generation wireless technology

FPGA : Field Programmable Gate Array

GA : Gaussian Approximation

3GPP : 3rd Generation Partnership Project

GPU : Graphical Processing Unit

IEEE : Institute of Electrical and Electronics Engineers

LAN : Local-Area Network

LCD : Leader of Converged Decoders

LDPC : Low Density Parity Check

LMA : LLR-Magnitude aided

LR : Likelihood Ratio

LLR : Log-Likelihood Ratio

MC : Monte Carlo

ML : Maximum Likelihood

mMTC : Massive Machine-Type Communications

MS : Min-Sum

Na-BPL : Noise-aided Belief Propagation List

NND : Neural Network Decoder

OCI : Observation of Consecutive Iterations

PKB : Perfect Knowledge Based

RM : Reed-Muller

RS : Reed-Solomon

RT : Round Trip

SC : Successive Cancellation

SCAN : Soft Successive Cancellation

SCL : Successive Cancellation List

SCS : Successive Cancellation Stack

SMS : Scaled Min-Sum

SNR : Signal-to-Noise Ratio

SR : Stochastic Resonance

3GPP : 3rd Generation Partnership Project

TSMC : Taiwan Semiconductor Manufacturing Company

uRLLC : Ultra-Reliable Low Latency Communications

WAN : Wide Area Network

WIB : Worst of Information Bits

XOR : Exclusive OR

CHAPTER 1

INTRODUCTION

"You don't understand anything until you learn it more than one way" – Marvin Minsky. I understood the importance of this sentence very well in my academic life. I have learned that this ability also contributes to the development of a good researcher. This thesis is the product of many hours spent re-reading my own draft manuscripts, trying to imagine how they would be viewed by others, evaluating, analysing, and rewriting them, all of which concluded in this thesis.

I started to my PhD studies on wireless communication theory over military HF protocols at TESLAB Gazi University in 2011. I worked with the physical layer design of military wireless communication systems which is consist of LDPC, Turbo, Golay channel coding, modulation scheme, channel estimation, equalization and HF channel modelling etc. I became a scholar of ASELSAN A.Ş within the scope of the project [1]. Working with expert engineers who have years of experience in the field has been extremely beneficial in developing my knowledge about communication theory. In addition to expanding my academic knowledge, I became more interested in wireless communication technology on a practical level. In this specific case, I encountered with FPGA technology. I projected that programmable integrated circuits (ICs) with high speed and parallel processing, such as FPGAs, would become more significant in the future for the implementation of algorithms such as channel coding and channel estimation. So, I began studying the VHDL programming language and progressed to the degree where I could help in lab courses at the university as a lab assistant, which was my goal. I've had the honour of advising undergraduate courses. This teaching has been extremely beneficial to me. I was able to work at the Optoelectronic and Nanoelectronics Laboratories (OPEN) and Optical and Photonics Laboratories (OFAL) labs at Çankaya University since I was able to put my theoretical knowledge into reality by implementing various FPGA

applications. These labs provided me with the chance to participate in a TUBITAK project on the design of underwater optical communication systems, which I completed by studying in there [2]. This project provided me with the chance to put my prior theoretical knowledge of FPGAs to use in a real-world setting. In addition, I actively participated in the implementation of the project that will provide financial support for Çankaya University to establish these labs. I produced eight publications as a result of working on these projects [6-13]. In addition to all these studies, I started to work as an application engineer on MATLAB and Simulink's communication, signal processing and digital design toolboxes in FİGES Engineering. I had the opportunity to work with all the leading companies of the defence industry in Turkey. In all this hard work, I was withdrawn from my PhD for neglecting one of the administrative processes. In the same year, the Turkish government introduced an academic amnesty. I made my re-registration and started working with my advisor Orhan Gazi. I owe my advisor a gratefulness for guiding me through the present PhD program. Based on my previous knowledge in the area of FPGAs, we developed a unique approach to the Polar encoding technique, which was then published [5]. Finally, we have proposed a communication system based on the Polar coding method, which includes my academic studies of the past 10 years. Basically, we suggested that frozen bits that are not used in polar coding should be used for channel estimation. We performed the performance analyses of this proposed system. As a result, this doctoral thesis contains the content of thirteen of my publications, which are included in the references [1-13]. Four of these have been published as research report [1-4] and three of them as journal paper [5-7]. The others are published as conference papers [8-13]. Computational theory of coding goes back to 1948, when Shannon released his article in which he stated the basic issue of how an information message may be delivered effectively and reliably through a noisy channel [14]. The solution to this query is referred to as "channel coding" by him. He did not go into details on how to design these codes, despite the fact that he demonstrated that such codes are possible. As a result, information theory and communication research have devoted most of their attention on discovering structures for practical coding schemes that are closer to Shannon's theoretical limits. Shannon showed that the coding issue may be divided into two different categories: source coding and channel coding. The first one’s role is to use as few bits as possible to

efficiently represent the information resource; the second's role is to offer redundancy in order to protect the information from the noisy channel and convey it reliably to be received. Shannon's channel coding theorem states that error free transmission can be achieved using channel codes for transmission rates below C (capacity). As the code length tends to infinity, there is a code sequence with a maximum probability of error that approaches zero. Many of the forward error correction (FEC) methods have been developed since the introduction of channel coding theorem. Some of the error-correcting codes that have been developed in the last 70 years are Hamming, low density parity check (LDPC), Reed-Solomon (RS), turbo, and polar codes. FEC methods are most commonly employed in wireless communication systems in order to improve the overall service quality of the network. Furthermore, different FEC algorithms are used for different frameworks ranging from 2G to 5G. All channel codes, from the simplest to the most complex, are created in a trivial way. To enhance the overall service quality of wireless communication networks, forward error correction (FEC) technologies are primarily used. Furthermore, different FEC algorithms are used for different frameworks, ranging from 2G to 5G in size and complexity. In polar codes, the probabilities of transmitted bits are related to the channel capacity available between the bit to be broadcast and the received symbols, as well as the previously decoded bits. These channel capabilities are often referred to as split channel capacities. Split channel capacities are used to determine the position of parity bits, also known as frozen bits, in polar codes, such that the locations of frozen bits are known by both the transmitter and the receiver at the same time. Locations of data bits and frozen bits are determined before the encoding procedure. Parity bits are created after encoding in all channel codes, with the exception of polar codes. The opposite is true with polar codes where, before encoding, parity bits i.e., frozen bits, are determined using the capacity of the split channels. Channels with limited capacities are employed to carry parity bits, whereas high-capacity channels are used to carry data bits. As a result of this intelligent channel utilization, polar codes outperform turbo and LDPC codes in terms of performance. Also, in his article [15], Arıkan described how to decode polar codes using successive cancellation decoding. In the years following their inception, polar codes have attracted the public's interest and have emerged as a key topic for future communication standards. Aside from that, polar codes were chosen to be used on the

control channels of the new radio (NR) of the third-generation partnership project (3GPP) [16], which is a third-generation partnership project. As it is shown in [17, 18, 19], polar codes may be utilized for both source coding and channel coding.

Within a short period of time after the introduction of polar codes, several decoding algorithms were developed. Multiple polar decoding approaches are now available, including successive cancellation (SC) [14], belief propagation (BP) [20], linear programming (LP) [21], and maximum likelihood (ML) [22]. In ML decoding, the probability of all potential codewords is determined for each codeword. After that, the most likely codeword is determined. Because ML decoding is based on finding all potential codewords, it becomes inapplicable beyond a certain codeword length N, because there is a total of 2^N possible codewords accessible, and for big N values, it becomes impossible to manage the number of computations required to decode the data. As a result of its practical relevance, SC decoding of polar codes is proposed in [15]. SC has poor error correction capability at short code lengths, whereas, the SC method has the lowest computational complexity of all the algorithms. The implementation of the SC list [23] decoder has significantly improved the performance of the SC decoder while keeping the complexity reasonable. It is presented in [20] as a generic form of the SC decoder, as well as its soft decision-based variant, and as a soft decision-based version of the SC decoder. It has been shown that polar codes exceed the performances of turbo and LDPC codes [24]. In [25], a full description of ASIC designs of Successive Cancellation (SC) decoders and other related topics were studied. [26] describes the implementation of a belief propagation (BP) decoder on a particular FPGA architecture. For punctured polar codes, it has been demonstrated that long length codes can be easily stored in flash memories for practical purposes. With the suggested encoding and decoding algorithms, many of the memory constraints that can arise during real applications with FPGA are considered in [27]. The main method to achieve this is to use puncturing. In addition, the fast Fourier transform (FFT) is performed using a parallel pipelined architectural method, which reduces the additional complexity associated with the operation. It is possible to minimize complexity by removing duplication [28-31]. The procedure is carried out in parallel for a variety of inputs, and it is discovered that the power efficiency is high. In November 2016, at the 3GPP RAN1# 87 conference in Las Vegas, the polar code coding

scheme was selected for the control channel coding scheme for the 5G eMBB (enhanced mobile broadband) environment [32]. After this conference, researches on polar codes focus on the 5G applications of polar codes [33-37]. These studies are restricted to 5G standard polar code which use basic polar rather than systematic polar, and the code length is limited to 1024 bits. Unlike all these studies, a unique coding method has been proposed instead of using the butterfly structure used in FFT and instead of using the huge number of BRAMs. Instead of using the high-capacity FPGA required in the 5G standard, the authors of [5] suggest a coding approach that may be simply implemented into novel communication systems.

On the other hand, the construction of polar codes for wireless communication channels presents significant difficulties due to the fading aspects and time-varying nature of the channel. Because of the growing need for remotely operated equipment, wireless communication has emerged as one of the most exciting research topics in recent years. There is also a bigger scale need for smart homes, satellite communications, and commercial and military applications that make use of smart house devices. As a result of this increased demand, researchers try to develop better and more dependable technologies. The theoretically proved performance of polar code makes this low complexity encoding scheme a promising technique for upcoming systems such as fifth-generation (5G) cellular services, which are under development. The third-generation partnership project (3GPP), an international standards body that develops telecommunication protocols, approved polar codes in 2006 for the control channels of the air interface, which is critical for 5G since they need a high data rate in order to operate. Due to the unpredictable and random nature of electromagnetic wave propagation in the air, which is the primary mode of wireless communication transmission, there are a variety of limits imposed by factors like as moving objects, the weather, and the huge mass of users. A shift in signal intensity over time and frequency is created by the former method, which is referred to as fading. The signal is duplicated in a fading channel, and the amplitudes, phases, and angles of arrival of the signal are all distinct from one another. This collection of duplicates is referred to as multiple pathways and it may be done in a constructive or harmful manner depending on the receiver. This multipath propagation environment fluctuates randomly and as a consequence, understanding the random

behaviour and offering methods to mitigate the negative impacts of fading have been among the fundamental parts of wireless communication channels for a long time. The authors of [47,50] suggest a method to obtain an improved design based on signal to noise ratio (design-SNR) for a given polar code structure using an optimization algorithm used for polar code structures. In order to address the performance loss caused by executing the codes at actual SNRs that are lower than the design SNR values, this solution has been developed: According to [47], for the two-block fading channel model with a binary-symmetric channel and an additional channel, a polar coding scheme is suggested using a binary-symmetric channel. When the instantaneous channel state information is not available at the transmitter, it is shown that the symmetrical capacities of the channels may be obtained. The estimation method is able to achieve good results in the AWGN channel [38]. It, on the other hand, does not perform well across fading channels. Several data-aided (DA) and non-data-aided (NDA) SNR estimate techniques are compared in [39]. The DA method provides precise estimate at the expense of high complexity; on the other hand, the NDA approach has a relatively low level of complexity while providing less accuracy. As an additional measure of efficiency, [40] proposes a modified technique based on the signal-to-variation ratio (SVR) to enhance estimating performance at the expense of increased complexity. Code-aided SNR estimate based on expectation maximisation (EM) for iteratively decoding the signal has been suggested in [41]. The frozen parts may also be referred to as pilots since they are completely transparent to both the sending and receiving sides of the transmission. The frozen bits may be used as DA without causing any bandwidth loss. However, all of the publications listed above have only looked into the estimate of SNR over an additive white Gaussian noise (AWGN) channel. An iterative maximum likelihood (ML) estimation algorithm of the log-likelihood function of the received signals has been proposed in [42] for fading channels; however, the computation cost of this recursive ML algorithm is extremely high when estimating the variance of posterior probabilities. For Rayleigh fading channel, model channel state information (CSI) is used at transmitter and receiver with proposed polar coding technique [43]. Furthermore, a recently published study [44] investigates the usage of polar codes in conjunction with bit interleavers (in order to boost the diversity gain) across two-block block fading channels. It is possible to categorize all of the accessible

research into two major types of study. In the first category polar coding methods use fading for their benefit, i.e., to increase diversity gain at the expense of communication latency [44,45,46].

Researchers for the second category consider fading as an issue and propose methods for mainly constructing polar codes for fading channels, which results in complex designs [43,47,48,49]. In our work, we have used a different method. With the help of the pilot symbol, we offer a straightforward and practical strategy that is based on channel inversion. For the pilot symbol, we utilized the frozen bits. In this case, the pilot insertion is being done in order to increase the performance of polar codes. The chosen pilots not only serve the goal of channel estimate or tracking, but they also help to secure transmission of the information by providing higher protection to the information bits. It is important to note that the modulation strategy used in this study is binary phase shift keying (BPSK). Therefore, we simply utilize pilot symbols, coded symbols, and pilot bits without giving them any attention. The thesis is divided into two parts: the first part is concerned with observing and improving the hardware design performance of the proposed polar encoding method by comparing it to the classical generator matrix-based encoding method; the second part is concerned with comparing the proposed polar encoding method to the classical generator matrix-based encoding method. The result was a more efficient coding structure that needs less space in any FPGA, resulting in increased efficiency. The suggested polar coding scheme is also studied for fading channels. The frozen bits are utilized to estimate the fading channel frequency response using the pilot-based channel estimation and the frequency domain channel equalization polar code, which are both implemented in the polar code.

CHAPTER II

POLAR CODE

As is well known, there are two kinds of channels: discrete and continuous. The continuous channel, which has two inputs and one output, is sometimes referred to as the analogue channel since it has two inputs and one output. In Fig. 2.1, the input signals $s(t)$, $n(t)$, and $r(t)$ represent the channel noise and the output signal, respectively.

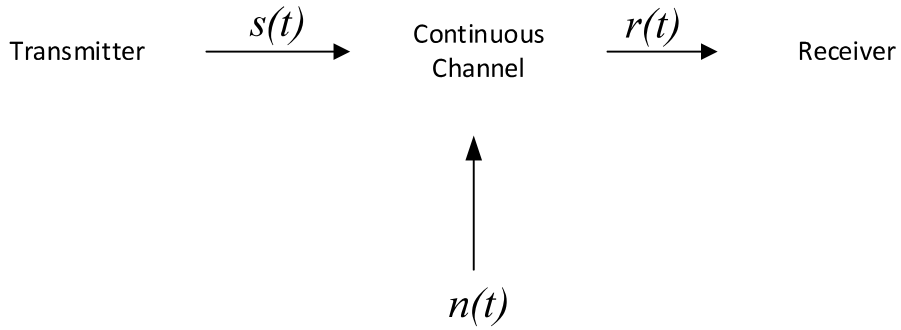

Figure 2.1 A continuous communication channel

The discrete channel on the other hand has both discrete input and discrete output. For this channel, if we wish to compute a probability on a bit-by-bit basis, the significance between X and Y may be stated as the transition probability, where input X is the input and Y is the output, as shown in Figure 2.2.

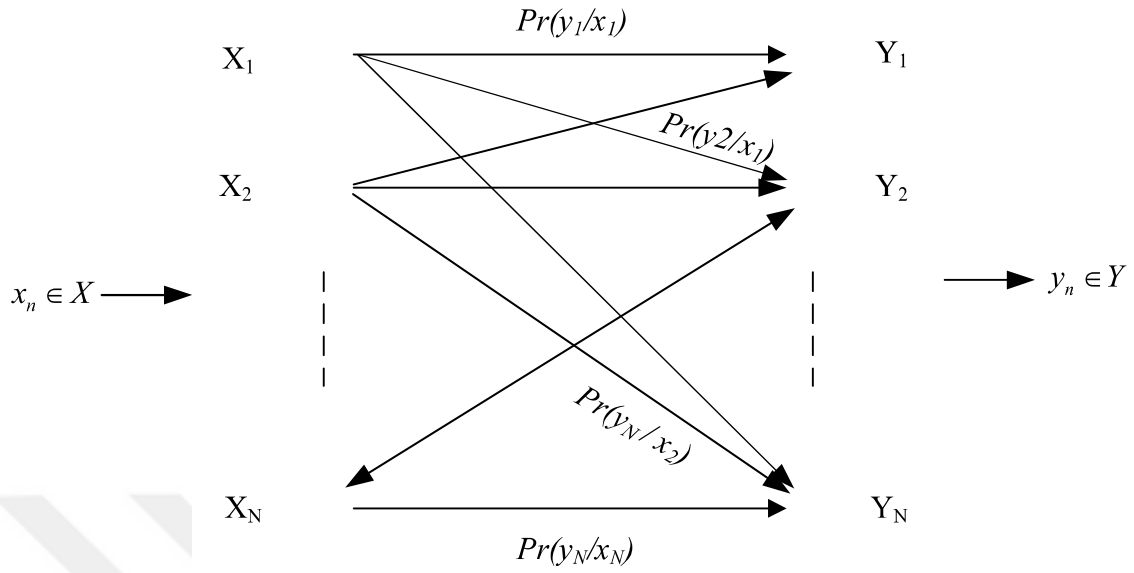

Figure 2.2 A sample discrete channel

The theory of polar codes and everything else may be described in a step-by-step manner. Polar codes are first used on binary-discrete memoryless channels [2]. The random variables u and y may be used to represent the input and output of a discrete memoryless channel denoted by W. In Figure 2.2 an n-input discrete memoryless channels (DMCs) are depicted.

1.1 CHANNEL POLARIZATION

With the mathematical model developed by Claude E. Shannon, it is possible to compute the channel capacity, which may be stated as the maximum mutual information between the input and output of a channel. Each polarized DMC has its own capacity ranging from 0 to 1. In other words, channel polarization allows us to create extreme channels by transforming non-zero capacity channels into extreme channels. These channels, which we also refer to as polarized channels, have no capacity or $C(W) = 1$ capacity, i.e., $0 \leq C(W) \leq 1$. Figure 2.3a and Figure 2.3b depict discrete memoryless

channels that are combined to form larger channels. The transformation matrix G, illustrated in Figure 2.3b, is referred to as the generator matrix of the polar code since it generates the polar code.

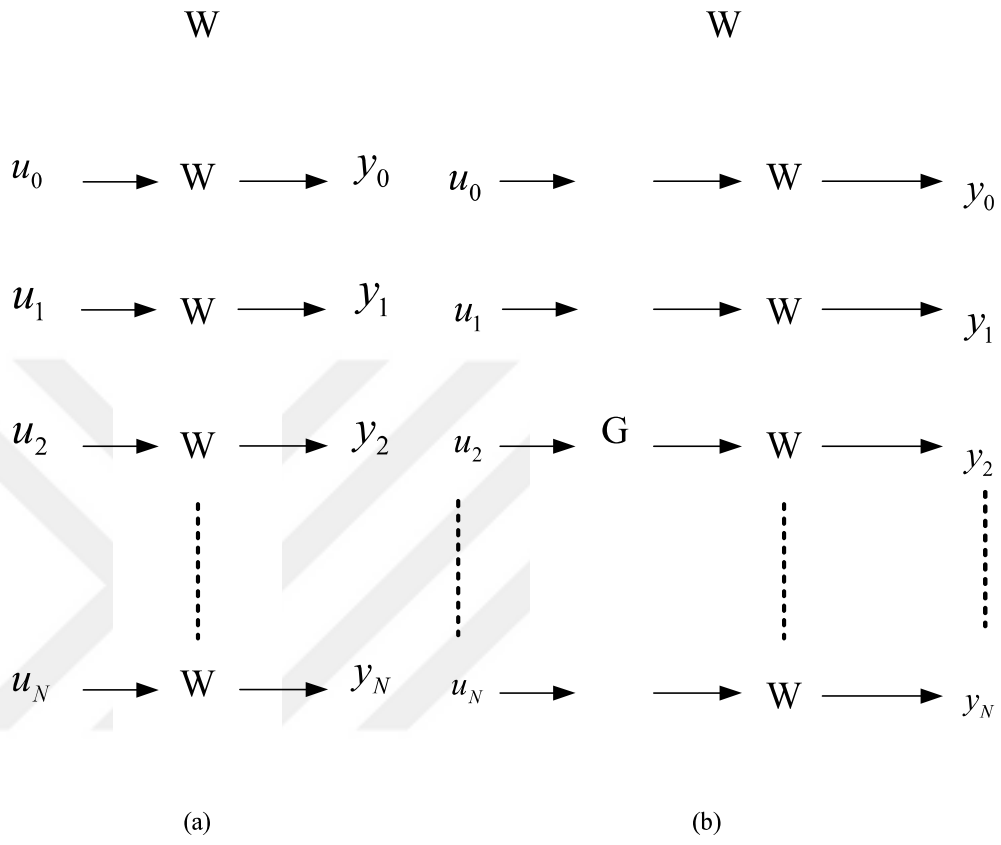

Figure 2.3 (a) Channel combining, (b) channel combining with channel polarization

Polar encoding can be performed simply by doing a modulo-2 addition, which can be accomplished using an exclusive-OR (XOR) gate. In the graphs shown in Fig. 2.4, the recursive channel combining operation is illustrated for $N = 4$. The binary-DMC (B-DMC) W_2 is formed by combining two binary-DMCs (B-DMCs) W_1^1, as illustrated in Figure 2.4a. In a similar manner in Figure 2.4b, two W_2 channels are combined to generate W_4. For codeword lengths that are powers of two, encoding can be done in a recursive manner.

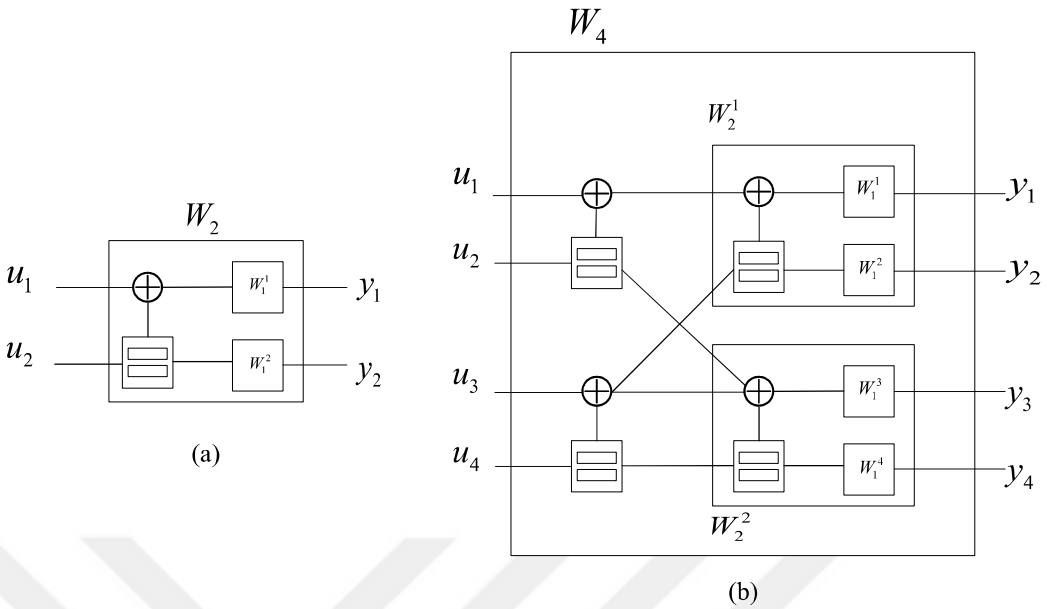

Figure 2.4 Channel combining examples (a) forming W_2 , (b) forming W_4

When the channel capacitances are polarized, the capacitances approach to 0 or 1, and this is desirable. Following an explanation of the concept of polarization, we will demonstrate how to generate a polar code for a Binary Erasure Channel (BEC).

Channel splitting should be used to see whether polarized channels have a different channel capacity than the original B-DMC W. As a summary, we may separate the combined channel into two sub channels and identify the B-DMCs that are bad and those that are good in the following ways:

$$W^+(y_1, y_2|u_1) = \frac{1}{2} \sum_{u_2 \in \{0,1\}} W_2\,(y_1|u_1 \oplus u_2) W_2(y_1|y_2) \tag{2.1}$$

$$W^-(y_1, y_2, u_1|u_2) = \frac{1}{2} W_2(y_1|u_1 \oplus u_2) W_2(y_2|y_2). \tag{2.2}$$

Using a variety of processes, a comparison of channel capacity before and after polar transformation might be expressed as in

$$C(W^-) \leq C(W) \leq C(W^+). \tag{2.3}$$

1.2 POLAR CODE CONSTRUCTION

The construction of polar codes is based on the kind of communication channel and decoder used. The purpose of a polar code is to polarize N independent copies of a given B-DMC channel to either 0 or 1. This will result in synthetic polarized channels. In order to measure the success of polarization, it is necessary to evaluate the quality of the channel. The Bhattacharyya parameter, which is denoted by the symbol $Z(W)$, can be used to evaluate the quality of synthetic channel output. We use Bhattacharyya parameter-based polar codes for BEC. It is critical to remember that information and frozen bit positions are decided before the polar code has been constructed. Frozen bit locations are often channels with zero or near-zero capacity that are known to the receiver and hence do not need to be retransmitted. The Bhattacharyya parameter can be defined as follows:

$$Z(W) \triangleq \sum_{y \in Y} \sqrt{w(y|0)w(y|1)} \tag{2.4}$$

where $y \in Y$ is the output symbol. As shown in Fig. 2.4, recursive operations can be utilized to generate polar code from a kernel code. The Bhattacharyya parameter can be determined recursively for split channels using;

$$Z(W_{2N}^{(i-1)}) = 2Z(W_N^{(i)}) - Z(W_N^{(i)})^2 \tag{2.5}$$

$$Z(W_{2N}^{(2i)}) = Z(W_N^{(i)})^2. \tag{2.6}$$

where it is seen that the recursive calculations begin by calculating the value of ${W_1}^i$ before proceeding further.

The success in polarization is dependent on the selection of ${W_1}^1$. Because we're dealing with BEC, we can set ${W_1}^1$ as the channel's erasure rate. For an erasure rate of 0.5 ${W_1}^1$ can be chosen as 0.5. The calculation of the Bhattacharyya parameters using a polar code is illustrated in Fig. 2.5.

It is seen from Fig. 2.5 that the Bhattacharyya parameter $Z(W)$ has large values for u_1, u_2, u_3 and u_5, and the others have smaller values. Using calculated values, we can decide that the best candidates for frozen bits are u_1, u_2, u_3 and u_5 which have the smallest capacity values, since $Z(W) + C(W) = 1$. Then, the data sequence to be encoded can be

written as $\boldsymbol{u} = [\, f\ f\ f\ d\ f\ d\ d\ d\,]$ where f and d denote frozen and data bits respectively.

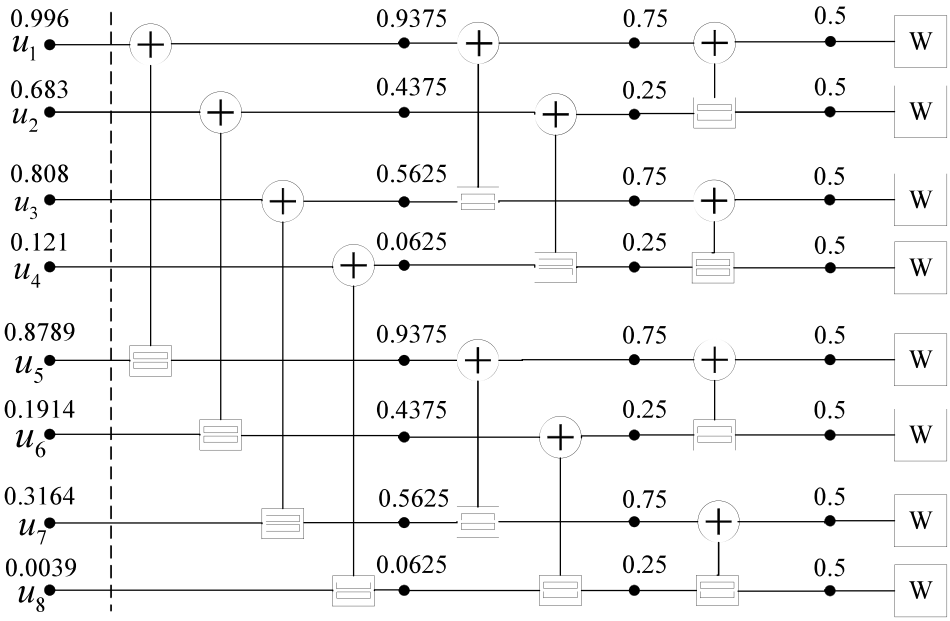

Figure 2.5 Bhattacharyya parameter based polar code construction for $N = 8$ [75]

Frozen bits are usually assigned the value of zero. After defining the frozen and information bit positions for an exact communication channel and decoder, our data sequence $\boldsymbol{u}$ is ready for encoding and transmission.

1.3 POLAR ENCODER

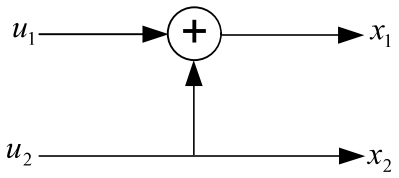

Figure 2.6 Polar encoder for $N = 2$

Fig. 2.6 depicts the polar encoder kernel unit where $x_1 = u_1 \oplus u_2$ and x_2=u_2 . After polar encoding, the resulting codeword for the information word $\boldsymbol{u} = [u_1 u_2]$ is $x =$

$[x_1 x_2]$, where $x_1 = u_1 \oplus u_2$ and x_2=u_2. When using any encoder, the relationship between $\boldsymbol{u}$ and $\boldsymbol{x}$ can be represented mathematically as

$$\boldsymbol{x} = \boldsymbol{u}\boldsymbol{G}_N \tag{2.7}$$

where $\boldsymbol{G}_N$ is the generator matrix. For N = 2, $\mathbf{G}_\mathrm{N}$ equal to

$$\boldsymbol{G}_2 = \begin{bmatrix} \mathbf{1} & \mathbf{0} \\ \mathbf{1} & \mathbf{1} \end{bmatrix} \quad \begin{matrix} \swarrow & \searrow \\ \boldsymbol{x_1 = u_1 \oplus u_2} & \boldsymbol{x_2 = u_2} \end{matrix} . \tag{2.8}$$

The generating matrix of the polar code is an involutory matrix, which means that it has the property:

$$\boldsymbol{G}_N = \boldsymbol{G}_N^{-1} \tag{2.9}$$

from which we get

$$\boldsymbol{x} = \boldsymbol{u}\boldsymbol{G}_N \rightarrow \boldsymbol{u} = \boldsymbol{x}\boldsymbol{G}_N^{-1} \rightarrow \boldsymbol{u} = \boldsymbol{x}\boldsymbol{G}_N. \tag{2.10}$$

$\boldsymbol{G}_N$ can be constructed in a recursive manner by starting with the mathematical equivalent of the kernel polar encoder unit illustrated in Fig. 2.6. The kernel matrix $\boldsymbol{F}$ is denoted by $\boldsymbol{F} = \begin{bmatrix} 1 & 0 \\ 1 & 1 \end{bmatrix}$. $\boldsymbol{B}_N$ is the permutation matrix referred to as the bit-reversal matrix and it is given as $\boldsymbol{G}_N$=$\boldsymbol{B}_N \boldsymbol{F}^{\otimes n}$ where $\boldsymbol{F}^{\otimes n}$ is the n^{th} Kronecker power of $\boldsymbol{F}$. $\boldsymbol{B}_N$ is recursively calculated using $\boldsymbol{B}_N$=$\boldsymbol{R}_N(\boldsymbol{I}_2 \otimes \boldsymbol{B}_{N/2})$ where $\boldsymbol{I}_2$ is the identity matrix and $\boldsymbol{R}_N$ is the permutation matrix, for instance and $\boldsymbol{R}_4$ transforms the input {1,2,3,4} to {1,3,2,4}.

In linear coder other than the polar codes, parity bits are inserted to the dataword to form the codeword when the G matrix is multiplied by the dataword. The dimensions of G matrix are $K \times N$ and $\boldsymbol{x} = \boldsymbol{u}\boldsymbol{G}$. The parity check matrix, $\boldsymbol{H}$, of the code satisfies $\boldsymbol{x}\boldsymbol{H} = 0$ where the size of $\boldsymbol{H}$ is $(N - K) \times N$. In polar coding, however, the $\boldsymbol{H}$ and $\boldsymbol{G}$ matrices are the same matrices of size $N \times N$. In addition, parity bits are inserted to the dataword before the encoding operation. Polar code with codeword length $\boldsymbol{N}$ and information bit vector length $\boldsymbol{K}$ is represented by $P(N, K)$.length $\boldsymbol{N}$ and information bits $\boldsymbol{K}$, $P(N, K)$.

CHAPTER III

FAST CALCULATION OF POLAR CODE BITS AND FROZEN-BIT LOCATIONS

3.1 INTRODUCTION

Polar codes are a class of channel codes designed in a non- trivial manner [14]. Polar codes are the first mathematically provable channel codes available in the channel coding world, and this can be considered as a major breakthrough in coding society. Polar codes have low performance at moderate and low codeword lengths. To improve the low performance of polar codes, the list and stack decoding algorithms are proposed [15,16,17,18]. Although, list and stack decoding algorithms show better performance than that of the classical successive cancelation method [19], they involve much more computations regarding the classical successive cancelation algorithm. Polar codes can also be decoded using a belief propagation algorithm [20]. In A. Andi, O. Gazi work [21], polar codes are concatenated with CRCs to prevent the performance degrading effect of error propagation. One other challenge on the implementation of these algorithms for future communication systems is the requirement of comprehensive digital electronic devices where hardware programming such as FPGAs stands as a strong candidate. The potential of FPGAs depends on the usage its resources efficiently. The encoding operation of the polar codes can be generated as the following formula,

$$x = uG \tag{3.1}$$

where u is the information word, x is code-word and G is the generator matrix. For $N = 1024$, and for full rate encoding operation, a binary generator matrix of size 1024×1024 should be stored in the memory units of the FPGA devices. Besides, if

different frame lengths are used for the transmissions such as $64, 128, 256, 1024, 2048$ etc., a generator matrix dedicated for each should be stored separately with different sizes in the memory units for efficient implementations. In this paper, we propose a method for the encoding of polar codes without the need for employment of generator matrix. The proposed method utilizes an n-bit binary counter, where $n = log_2(N)$, and a tree structure [22] involving n levels. Since the proposed method avoids the use of generator matrix, a smaller memory space in FPGA is required which reduces the hardware complexity of the polar encoders. Using the proposed method, it is also possible to calculate the code bits in parallel at the same instant. Split channel parameters such as Bhattacharyya bounds or average- bit-error probabilities are used for the determination indices of data and frozen bits. We proposed a tree-based approach for the calculation of split channel parameters in an efficient manner. Using the proposed approach, it is possible to calculate the all-split channel parameters such as Bhattacharyya parameters of all the bits which can be transmitted at the same time in a parallel manner.

3.1.1 Polar Encoding with Generator Matrix

In this section, we review the construction of the generator matrix, and polar encoding operation with generator matrix. Let's denote the N-bit information vector by

$$u_0^{N-1} = (u_0, u_1, \cdots, u_{N-1},) \tag{3.2}$$

The Polar code-word for the data vector u_{N-1} is obtained using

$$x_0^{N-1} = u_0^{N-1}\, G \tag{3.3}$$

where the generator matric G_N is calculated via

$$G_N = B_N F^{\otimes n} \tag{3.4}$$

in which $N = 2^n$, $F = \begin{bmatrix} 1 & 0 \\ 1 & 1 \end{bmatrix}$ and B_N is found using

$$B_N = R_N\left(I_2 \otimes B_{N/2}\right) \tag{3.5}$$

where the initial value of B_N, i.e., B_2 is I_2, and R_N denotes the $N \times N$ reverse shuffle permutation matrix whose operation is explained in

$$(s_0, s_1, s_2, \cdots, s_{N-1})\, R_N = (s_0, s_2, s_4, \cdots, s_{N-2})(s_3 \cdots, s_{N-1}) \tag{3.6}$$

The Kronecker product of two matrices $A = [\cdot]_{m\times n}$ and $B = [\cdot]_{k\times l}$ is obtained as

$$A \otimes B = \begin{bmatrix} A_{11}B & \cdots & A_{1n}B \\ \vdots & \ddots & \vdots \\ A_{m1}B & \cdots & A_{mn}B \end{bmatrix} \tag{3.7}$$

and the Kronecker power is defined as

$$A^{\otimes n} = A \otimes A^{\otimes(n-1)} \tag{3.8}$$

Graphical Illustration of Polar Encoding:

The encoding operation for $N = 4$ to obtain the code bit x_0 and its tree representation are graphically illustrated in Fig. 1.

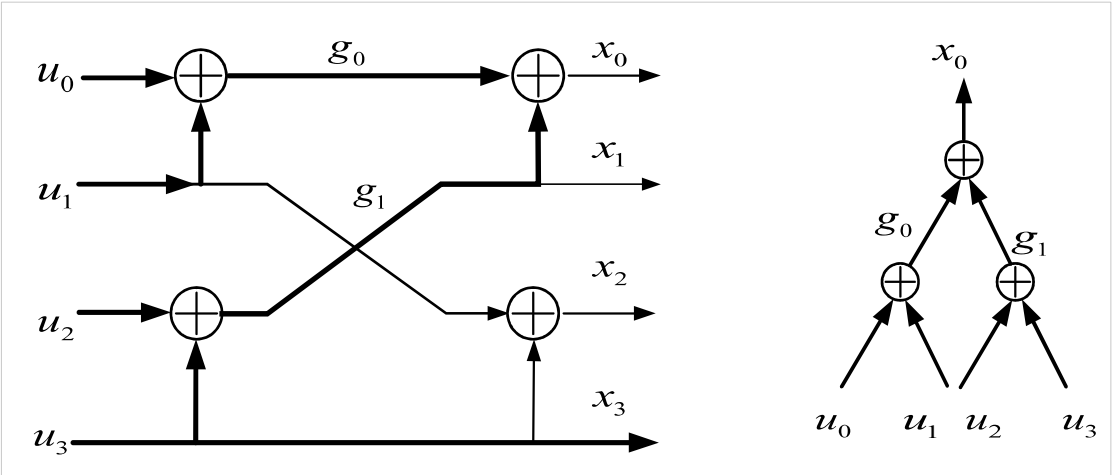

Figure 3.1 Encoding path and tree structure of the codeword symbol x_0.

3.1.2 POLAR ENCODING WITHOUT THE EMPLOYMENT OF GENERATOR MATRIX

Inspecting the encoding operations in Fig. 1 and its trellis representations, we propose a polar encoding operation without the employment of the generator matrix as follows. Pass-nodes in the encoding tree are defined as the nodes which only take the right incoming input bit from the lower layer. Sum-nodes in encoding tree are defined as the nodes which produce the mod-2 sum of the left and right incoming input bits from the lower layer. An n-bit counter is used for the encoding operation. The'1's in the n-bit counter indicate the levels which include pass nodes, and 0's in the n-bit counter indicates the levels which include sum-nodes. The n-bit counter is initialized to all zero tuples, and it is incremented at the calculation of each succeeding code-bit. The least significant bit of the counter indicates the top-level in the tree structure, and the most significant-bit of the counter indicates the bottom level of the tree structure. As an example, for $N = 8$ in Fig. 2, the generation of the code bit x_6 is illustrated. The counter has the value of 110 and, the '1's in the counter indicates the levels 1 and 2 where the nodes are pass-nodes. The propagating signals are shown using bold arrows.

For $N = 1024$, we need an $n = \log_2(1024) \rightarrow n = 10$-bit counter, and there are 10 levels in the tree structure, and using the $n = 10$-bit, and tree structure the encoding operation can be performed in a fast manner without requiring the generator matrix. The encoding algorithm using tree structure and counter is defined below.

Proposed Encoding Algorithm:

1. Initialize n-bit, where $n = \log_2(N)$ counter to all zeros and set $k = 0$.
2. The code-bit $x_k = 0 \ldots N - 1$, is to be generated, and n-bit counter has the binary equivalent of k.
3. Decide the levels corresponding to the positions of '1's in the counter such that the least significant bit of the counter points to the top level, i.e., level-0. The nodes of those levels corresponding to the positions of '1's of the counter is labelled as the pass-nodes, and the others are labelled as sum-nodes.
4. Starting from the lowest level above the ground level, OR the bit pairs coming from the predecessor level if the level has label '0', otherwise, just pass the right

incoming bit to the upper-level, and repeat this process till the top-most level and obtain the code bit x_k.

5. If $k = N - 1$ terminate, otherwise, increment the k value and go to step-1.

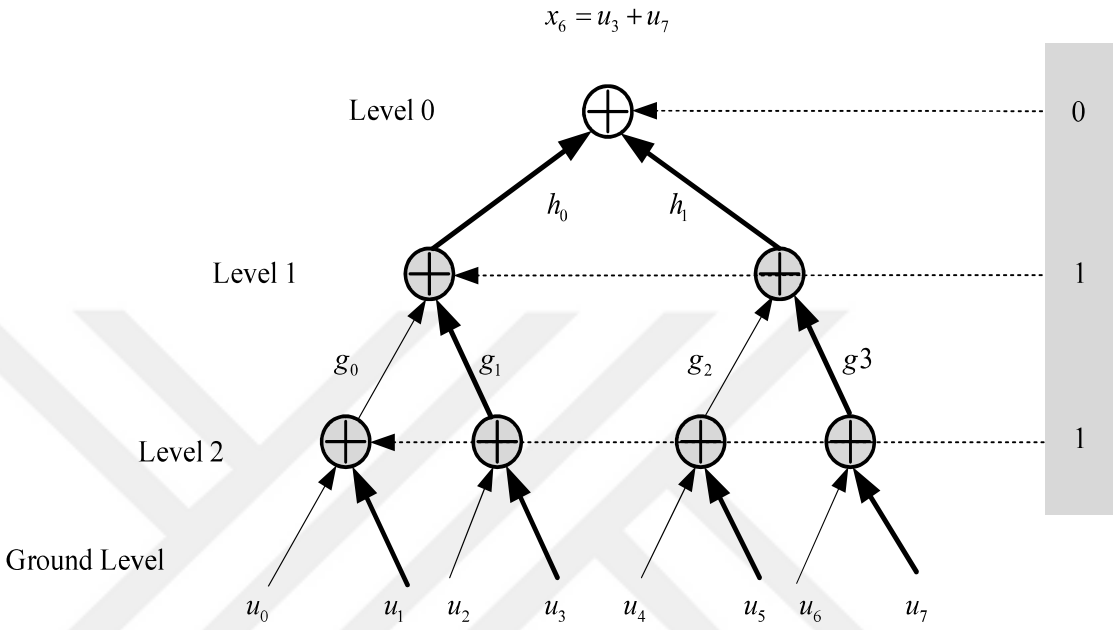

Figure 3.2 Proposed method encoding structure of x_6.

Example: For $N = 16$, the generation of the code bit x_{13} is illustrated in Fig. 3, where the 4-bit binary counter has the binary value 1101 whose decimal equivalent is 13.
As it is seen from Fig. 3 that for code bits with odd indices, only the right-hand side of the tree can be used, and this further decreases the complexity of hardware implementation.

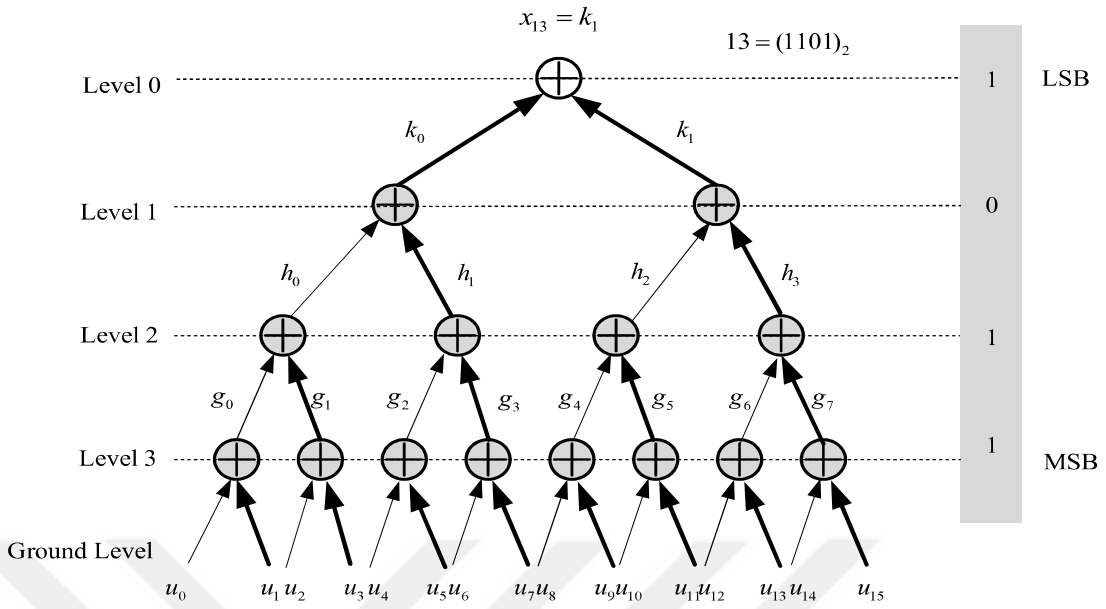

Figure 3.3 Example for tree-encoding operation.

It is also possible to generate all the code bits at the same time using the proposed tree-encoding structures in parallel. Since, the counter **values** are known and many of the tree-encoding structures can run in parallel, encoding operation can be completed by all parallel units at the same time. This approach reduces the encoding latency significantly; however, the hardware complexity increases.

3.1.3 Calculation Of Maximum/Average Bit-Error Probability Using Three Structures

In polar codes, the location of the frozen bits, i.e., parity bits are decided using the split channel capacities which are calculated before the encoding operation. Large capacity channels are used for the transmission of data bits whereas low-capacity channels are used for frozen bits. Location of frozen and data bits should be written into memory units to be used during the transmission and if the environment changes such as in the wireless communication, these split channel capacities should be re-calculated and written into memory locations again. For binary erasure channels, it is possible to calculate the split channel capacities exactly. However, for other channels, especially for wireless channels, the calculation of channel capacities is not a straightforward process and for most of them, explicit methods are not defined in the literature. The capacity of a split channel is closely

related to the average- bit-error probability of the transmission performed through the channel under concern, and Bhattacharyya parameters corresponding to bounds of maximum probability of bit errors can be used for this purpose. For polar codes, the Bhattacharyya parameters corresponding to maximum probability of bit errors are calculated in a recursive manner as in

$$\begin{aligned} &Z\left(W_{2N}^{2i-1}\right) \leq 2Z\left(W_N^i\right) - Z^2\left(W_N^i\right) \quad i = 0, \dots, N-1 \\ &Z\left(W_{2N}^{2i}\right) = Z^2\left(W_N^i\right). \end{aligned} \tag{3.9}$$

The locations corresponding to large and small Bhattacharyya values are chosen for frozen and information bits, respectively. It is seen from (3.9) that Bhattacharyya parameters are calculated in a serial manner. Considering the fact that reprogrammable hardware devices such as FPGAs will be idly used in the future communication technologies, split channel capacities or Bhattacharyya parameters can be calculated by such digital devices.

In this part, we propose a method to calculate Bhattacharyya parameters or maximum/average bit-error probabilities of the transmitted bits using tree structure in a parallel manner. With the proposed method, Bhattacharyya parameters or maximum/average bit-error probabilities can be calculated in an efficiently and a decision can be made whether the bit corresponds to a frozen or data bit. Using the proposed method, the calculation of the maximum or average bit error probabilities for all split channels can also be performed at the same time in a parallel manner and defining a threshold pte for the transmission error probabilities, those bits having maximum/average transmission error probabilities below a threshold value can be transmitted which can provide an uninterrupted transmission. For instance, if we take the threshold value $p_{te} = 0.4$ then for a new channel, the information bit u_i is transmitted if its calculated maximum/average bit error probability, related to the split channel capacity, is smaller than p_{te}, i.e., if $p_e < p_{te}$.

3.1.3.1 Proposed Method

In this subsection we explain the proposed method with an algorithm for the determination of bit error probabilities of split channels:

1) Initialize the counter to all zeros and set $k = 0$.
2) The maximum or average bit-error probability is to be calculated for the bit u_k, $k = 0 \ldots N - 1$ and n-bit counter has the binary equivalent of k.
3) Decide the levels corresponding to the positions of '0's and '1's in the counter and assign the counter bits to the tree levels such that the least significant bit of the counter points to the top level, i.e., level-0.
4) Starting from the level above the ground level, combine the α terms where α terms can be Bhattacharyya parameters or they can be average bit-error probabilities, and use $f(x) = 2x - x^2$ if the level label is zero or use $g(x) = x^2$ is the level label is 1, and repeat this till the top most level and obtain the maximum/average probability of error bit uk.
5) If $k = N - 1$ terminate, otherwise, increment the k value and go to step-3.

The graphical illustration of the proposed approach for the calculation of maximum/average bit error probability for u_{13} is depicted in Figure 3.4 where $g(\cdot)$ function is employed for the nodes belonging to the levels whose bit label is '1', whereas $f(\cdot)$ function is employed for the nodes belonging to the levels whose bit label is '0'. In Figure 3.4, except for the nodes in level-1, $g(\cdot)$ function is utilized for all the other nodes. A numerical example for the calculation of Bhattacharyya value for u_{13} for binary erasure channels with erasure probability $\alpha = 0.5$ is depicted in Figure 3.5 where it is seen that the output of the top node is 0.015 defined as the maximum probability of bit error for the bit u_{13}. Here, due to such a small maximum bit error probability, the bit u_{13} can be chosen as information bit, i.e., bit location 13 can be reserved for information bits.

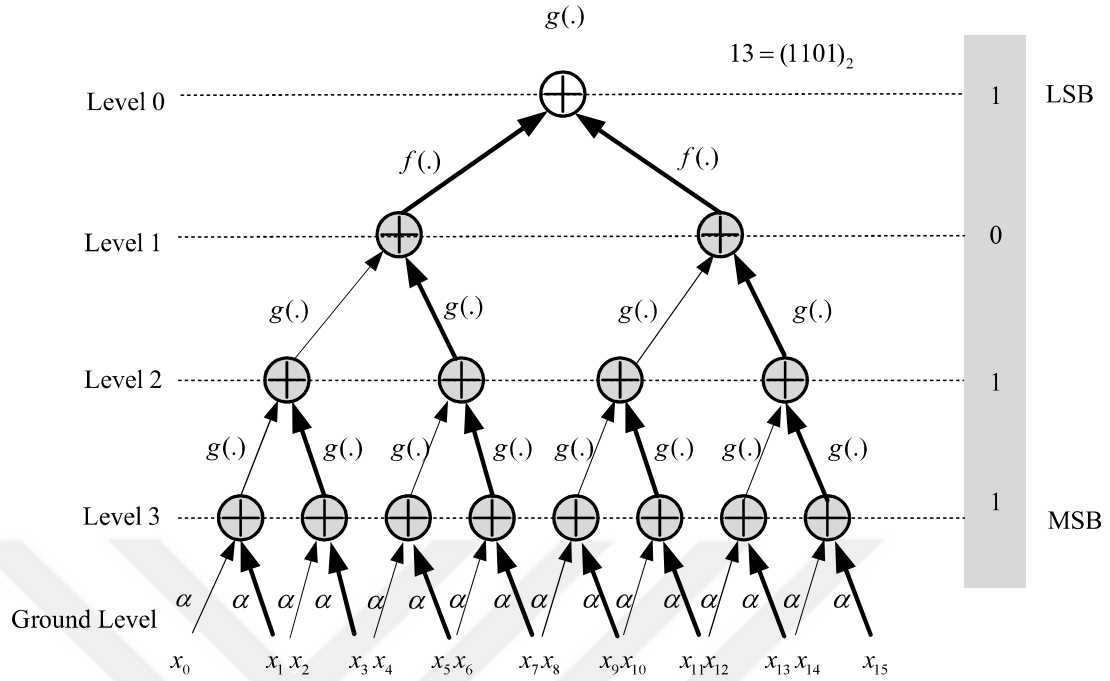

Figure 3.4 Maximum/average bit error probability calculation for u_{13}.

The tree structure shown in Fig. 5 can be constructed for all the data bits, since the counter values can be known enabling parallel calculation of all the split channel parameters.

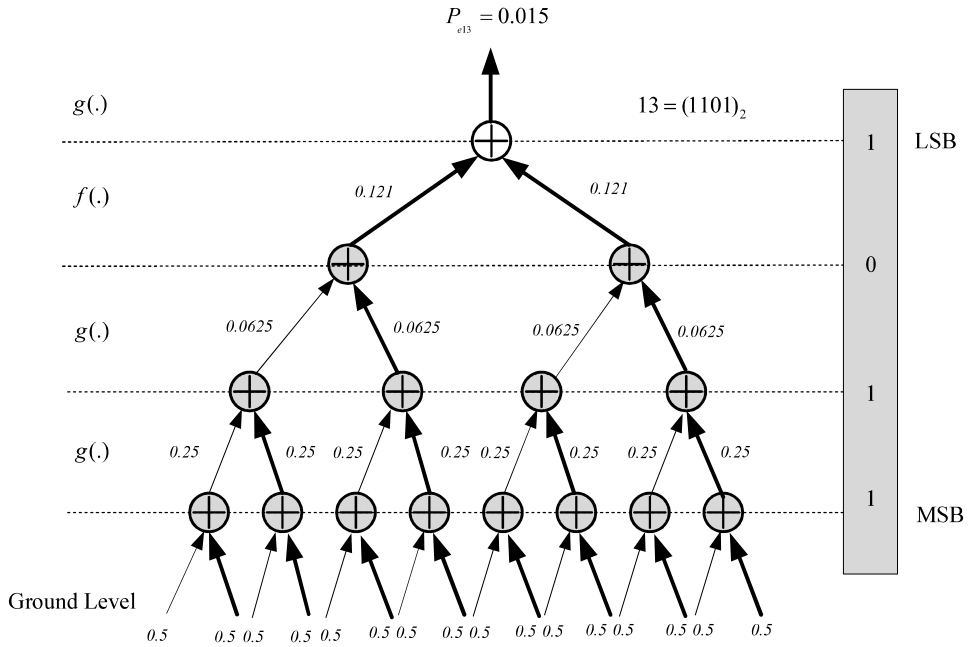

Figure 3.5 Calculation of Bhattacharyya value for u_{13} for BEC with $\alpha = 0.5$.

3.1.4 Implementation Results

In this section, we provide information about the hardware space consumption of the proposed techniques and make a comparison with the classical approaches. The polar encoding using the generator matrix and proposed algorithm are compared in Table-3.1 and Table3.2 in terms of the digital resources used. For the classical polar encoding, we used the formula $x = uG$, and the rows of G matrix corresponding to the positions of '1's in u vector are XORed. Both algorithms are implemented by using an Nexys-3 spartan-6 FPGA board. It is seen from the table that as the frame length increases the hardware requirement of the proposed method favours significantly over the classical one where for frame length $N = 1024$, the proposed approach uses three times less hardware resources.

Table 3.1 Hardware Consumption (Number Of Slice Registers (NOSR))

Logical Utilization	**Proposed Polar Encoder N=8**	**Proposed Polar Encoder N=16**	**Proposed Polar Encoder N=32**	**Proposed Polar Encoder N=64**
Generic Method LUTS	11	22	46	112
Proposed Method LUTS	10	19	36	69
Logical Utilization	**Proposed Polar Encoder N=128**	**Proposed Polar Encoder N=256**	**Proposed Polar Encoder N=512**	**Proposed Polar Encoder N=1024**
Generic Method LUTS	261	586	1312	3136
Proposed Method LUTS	135	266	524	1038

The consumed hardware space gain of the proposed approach is depicted in Fig. 3.6 where it is seen that for frame length $N = 1024$ the proposed method gains 70% hardware space, i.e., if the classical approach consumes 100 hardware resources, the proposed method consumes only 30 hardware resources.

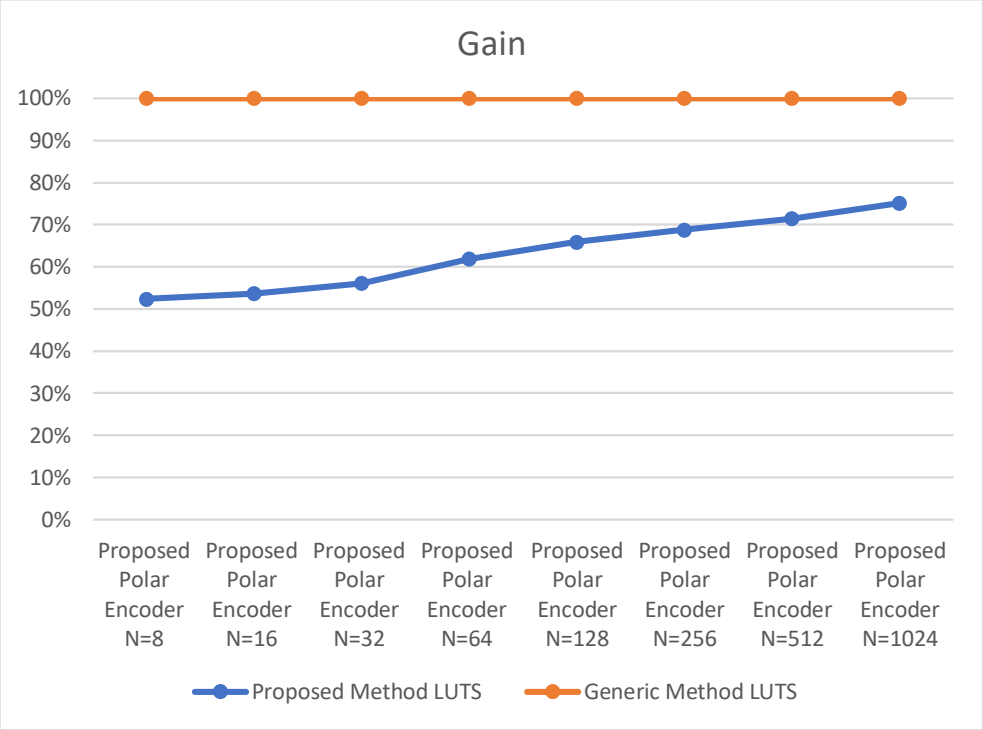

Figure 3.6 Comparison of hardware space consumption gain for the proposed and classical encoding approaches.

In this chapter, we proposed tree-based structures for the encoding of polar codes without the use of a generator matrix, and for the calculation of split channel parameters which are used for the classification of bits to be transmitted as data or frozen bits. The suggested structures are suitable for sequential and parallel processing operations. It is also shown that using the proposed methods, it is possible to calculate the polar code bits, and split channel parameters at the same instant in a parallel manner. When the suggested structures are implemented in hardware using digital electronic devices, they consume less hardware space and work faster.

Table 3.2 All Hardware Consumption

Logical Utilization	N=8	N=16	N=32	N=64	N=128	N=256	N=512	N=1024	N=2048
Number of Slice LUTs	10	19	36	69	135	266	524	1038	2064
Adders/Subtractors	1	1	1	1	1	1	1	1	1
Registers	8	16	32	64	128	256	512	1024	2048
Muliplexers	7	15	31	63	127	255	511	1023	2047
Xors	7	15	31	63	127	255	511	1023	2047

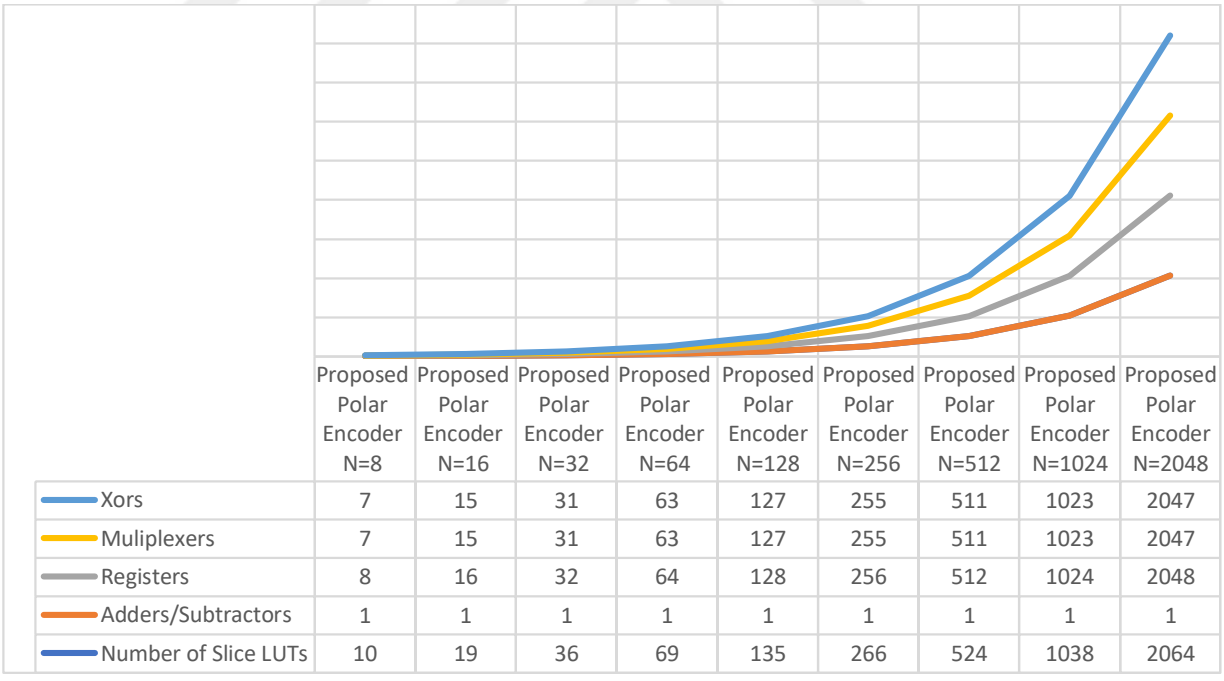

	Proposed Polar Encoder N=8	Proposed Polar Encoder N=16	Proposed Polar Encoder N=32	Proposed Polar Encoder N=64	Proposed Polar Encoder N=128	Proposed Polar Encoder N=256	Proposed Polar Encoder N=512	Proposed Polar Encoder N=1024	Proposed Polar Encoder N=2048
Xors	7	15	31	63	127	255	511	1023	2047
Muliplexers	7	15	31	63	127	255	511	1023	2047
Registers	8	16	32	64	128	256	512	1024	2048
Adders/Subtractors	1	1	1	1	1	1	1	1	1
Number of Slice LUTs	10	19	36	69	135	266	524	1038	2064

CHAPTER IV

FREQUENCY DOMAIN CHANNEL ESTIMATED POLAR CODING OVER FADING CHANNEL

Arıkan introduces polar codes in [15], that are the first theoretically verified error correcting codes capable of reaching Shannon's capacity. Following its introduction, polar codes have been accepted for usage in the uplink and downlink control channels of the 5G framework of eMBB, which was introduced by the 3GPP group [16]. Polar codes may be decoded using a range of different methods. In [15], Arıkan presents the first decoding method, the SC decoding algorithm, for generic channels, which is still in use today. There are other decoding techniques suggested in addition to the SC decoding algorithm, including CRC-aided SC List [23] decoding, belief propagation (BP) based decoding [20], SC stack (SCS) decoding [24], and linear programming (LP) based decoding of polar codes [21]. According to [23], it has been demonstrated that polar codes with CRC assisted SCL decoding beat the maximum probability limit of polar code with a high list size and can compete with LDPC codes. However, SC and SCL decoders, on the other hand, disadvantage from their serial character. Arıkan [20] proposes a BP algorithm-based polar decoder as a means of overcoming this limitation and providing academics with a new point of view. The capacity to decode bits in parallel is the fundamental characteristic of the BP polar decoder. Despite the fact that BP decoders have a larger degree of complexity than SC-based decoders (SCL and SCS), their throughput performance is exceptional when compared to the state-of-the-art SC-based decoders.

Even though the study on polar codes and fading channels has previously been done, it is not particularly recent. It is primarily the work of Liu, Hong, and Viterbo that has provided the fundamental motivation [52]. It is suggested that fading channels are

naturally polarized because the chance of distortion in a fading channel is directly proportional to the channel gain (or fading coefficient), and this phenomenon is known as "fading polarization.". They present a novel approach for estimating the Bhattacharyya parameters that is adapted particularly for fading channels, allowing them to better fit the polar code design to fading channels than previous methods.

At a block error rate of 10^{-4}, it is discovered that this approach provides a 1.5 dB gain over LDPC codes. Bravo-Santos developed a new polar coding method based on channel characteristics. This method is found to be effective on both binary input and block Rayleigh fading channels, respectively. According to the results, when high codelengths are utilized, the proposed technique is closer to the theoretical limit than Turbo and LDPC codes [54].

Trifonov design the polarized subchannels over wireless fading channels with returns that also have Chi(χ) distribution where is a usual form of Rayleigh distribution. It should also be observed that this kind of modeling may be utilized to predict the error probability in the polarized subchannels. It is also noted that polar codes underperform in the fading channels when they are not tuned for the Rayleigh channel. Sequential or list decoding is used to effectively to set the frozen bits in linear combinations. In the latter scenario, it is shown that the usage of dynamic frozen symbols results in a considerable performance improvement over equivalent LDPC code [55].

Boutros and Biglieri continue their discussion of block fading channels by stating that, unlike the fundamental design of polar codes. The channel polarization in block fading channels may be considered of as several parallel channels with differing mutual information [45]. The authors suggest a hierarchical polar coding system for fading binary symmetric which is similar to the work of Boutros and Biglieri. However, the authors do not use CSI at the transmitter [47]. Bravos-Santos and Trifonov restrict the Rayleigh fading channel and examine the polar code [55]. Because of the inherent nature of wireless transmission, employing polar codes for telecommunication across fading channels presents a number of difficulties. This is due to the fact that the wireless communication channel varies over time and that polar coding is essentially channel specific in nature.

In this thesis transmitting polar coded data over wireless fading channels which is combined with channel estimation and equalization approaches are improved the

performance. There has been some early research on polar coding techniques that can achieve the capacity of AWGN channel [50]. In recent research [52], the channel specific character of polar codes was taken into account. According to the authors, they have developed a heuristic technique that may be used to achieve an optimum design SNR for a particular polar code structure.

In the condition of fading channels, [52] proposed a polar coding system for two block fading channel models to be used in combination with each other. Without any initial information of the channel condition at the transmitter, it is shown that the technique is capable of achieving the symmetric capacities of the channels.

It is possible to categorize all of the accessible research into two major types of study. Among the first are studies that offer polar coding methods to take use of fading to their advantage, i.e., to enhance diversity benefits at the expense of transmission latency [45,47]. Fading is treated as a barrier in the other group of studies [44, 48, 49,52,53] and they offer strategies to specifically develop polar codes for fading channels, which often results in complicated designs. We have adopted a different approach to the problem.

We propose a basic practical scheme channel estimation and equalization utilized with the polar codes frozen bits distributions to use polar codes in a fading channel. The method has the advantages for the irrespective channel situation. Using the frozen bits suffices for the channel estimation and with the frequency domain channel equalization communication is improved under the fading channel.

In section 4.1 Bhattacharyya parameter based polar code design is presented. In section 4.2, channel estimation and equalization methods are introduced. Finally, in section 4.3, channel estimated and equalized polar decoder are studied and a comparison with SC-based polar decoding are shown.

4.1 BHATTACHARYYA PARAMETER BASED POLAR CODE DESIGN

As an analytical approach, Bhattacharyya parameter [15] is a well-defined for the SC-based polar decoder for the binary erasure channel (BEC). Different decoders with different channel types cannot achieve optimal BER/BLER performance due to the absence of well-defined polar code construction methods [58]. To cover this deficit, some methods that relies on both analytic methods like density evolution (DE) [59], and

Gaussian approximation for DE [60], and MC based designs [53, 61, 62, 63] are introduced.

Among the polar code construction methods Bhattacharyya parameter-based construction is utilized in thesis [15] and also combined with the channel estimation and frequency domain channel equalization methods [64-71].

Bhattacharyya parameter-based estimation is designed for binary erasure channel, and it is not the optimum construction method for AWGN, Raleigh fading channels etc. Bhattacharyya parameter of a binary-discrete memoryless channel denoted by W is defined as

$$Z(W) \triangleq \sum_{y \in Y} \sqrt{w(y|0)w(y|1)} \tag{4.1}$$

where $y \in \mathrm{Y}$ is an output alphabet. The value of $Z(W)$ is closely related with the capacity of a channel, $C(W)$, such that $C(W) + Z(W) = 1$. Recursive calculations are performed to compute the channel capacities Bhattacharyya parameters as

$$Z(W_{2N}^{(i-1)}) = 2Z(W_N^{(i)}) - Z(W_N^{(i)})^2 \tag{4.2}$$

$$Z(W_{2N}^{(2i)}) = Z(W_N^{(i)})^2 \tag{4.3}$$

An example of combining channels is depicted in Figure 4.1.

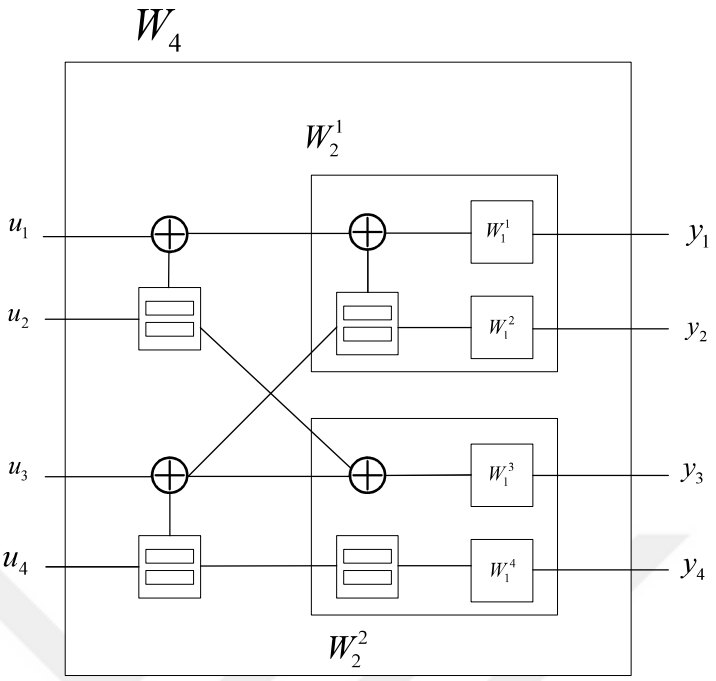

Figure 4.1 Combining channels to get polarized channels

For the rightmost side, we have $W_1^i = W$ where $1 \leq i \leq N$. Erasure probability of the BEC can be used directly for W_1^i. However, initial value of Bhattacharyya parameter is difficult to find for Gaussian and Rayleigh channels since both channels are continuous. We prefer to use a practical construction method of polar codes in AWGN channels [74]. In [74], initial value of W_1^i is determined by bit error probability P_e of AWGN channel defined as $P_e\left(\frac{R_s R_s E_b}{N_0}\right)$ where R_s is symbol rate, R_c is code rate and E_b/E_0 is the energy per-bit. We use BPSK and AWGN channel, that is R_s is 1 and the code rate is generally set to 0.5. It is important to state that the value of E_b/E_0 in dB scale is always set to 0.5 dB, the design SNR, for the simulations of this thesis, unless otherwise indicated.

As an example, frozen bit distribution for $\mathcal{P}(2048,1024)$ and $\mathcal{P}(1024,512)$ are calculated for both BEC and AWGN channels and frozen bit locations are illustrated in Figure 4.2, Figure 4.3, Figure 4.4 and Figure 4.5.

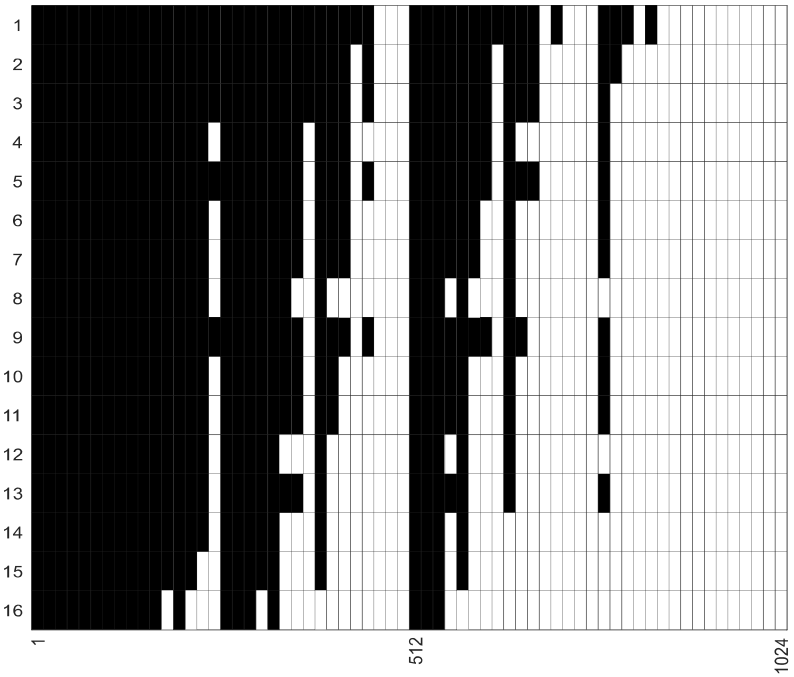

Figure 4.2 Frozen bit locations of $\mathcal{P}(1024,512)$ erasure probability BEC at 0.5 dB [75]

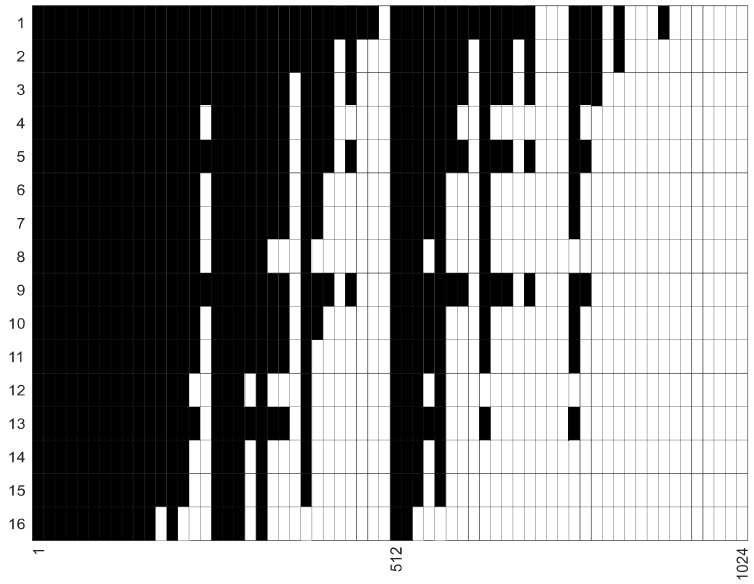

Figure 4.3 Frozen bit locations of $\mathcal{P}(1024,512)$ for AWGN with design SNR of 0.5 dB [75]

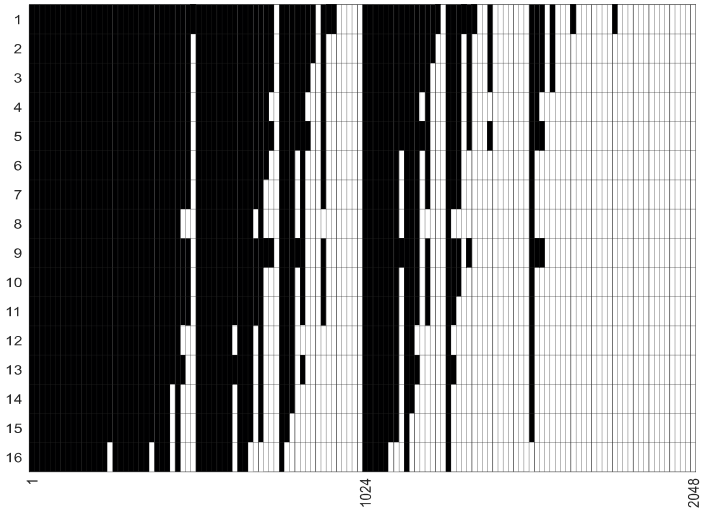

Figure 4.4 Frozen bit locations of $\mathcal{P}(2048,1024)$ erasure probability of BEC at 0.5 dB [75]

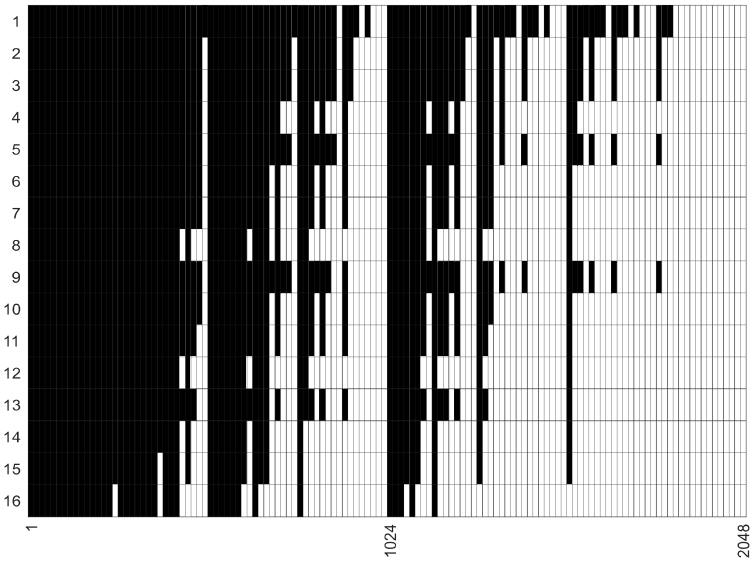

Figure 4.5 Frozen bit locations of $\mathcal{P}(2048,1024)$ for AWGN with design SNR of 0.5 dB [75]

Table 4.1 contains a summary of the original Bhattacharyya parameters, as well as the channel capacity for comparison. Due to the AWGN channel's initial parameter's

dependence on the noise variance we shall refer to it in Table 4.1 as the AWGN ($\sigma 2$) parameter.

Table 4.1 Bhattacharyya parameters of different channels

	Capacity	Initial Bhattacharyya parameter
BSC(p)	$1 - \mathrm{H}(p)$	$2\sqrt{p(1-p)}$
BEC(ϵ)	$1 - \epsilon$	ϵ
AWGN(σ^2)	(½)$\log_2(1+E_s\sigma^2)$	$e^{-Es\sigma^2}$

Polar codes are those that make use of the polarization effect in some way. As previously explained, the basic concept is to transfer data over good channels with capacities that trend to 1, while freezing data over poor channels with capacities that trend to 0. Polar code is described as $(N, K, \mathcal{A}, u\mathcal{A}c)$. In the definition of a polar code the following parameters are used: $N = 2n$ for the codelength, K for the number of information bits, $\mathcal{A}$ is the information set. In this thesis we use all-one vectors for the frozen bits. We only use channels with the fewest Bhattacharyya characteristics while transmitting data. $N - K$ bits of the set $\mathcal{A}c$ are used to store the values and channels of all of the frozen variables that are known to the receiver.

4.2 CHANNEL ESTIMATED AND EQUALIZED-BASED POLAR DECODER

4.2.1 The Wireless Fading Channel

As it is known, electromagnetic waves are responsible for the operation of signals over a wireless channel. Assuming the system is coherent we may designate the banspass signal input as $s(t) = \Re\{u(t)e^{j}2\pi f_c t\}$ where $u(t)$is the amplitude of $s(t)$ and f_c is the carrier frequency of the input signal. Because of reflection, diffraction, and dispersion, there are several possible pathways for a single sent signal, each with a different delay and Doppler phase shift than the previous path. The final received signal is sum of the faded and delayed of the transmitted signal as:

$$r(t) = \Re\left\{\sum_0^{N(t)} \alpha_n(t)u(t-\tau_n(t))e^{j2\pi[f_c(t-\tau_n(t))+\phi D_n]}\right\} \quad (4.4)$$

n is the index of the path, $\alpha_n(t)$ is the attenuation coefficient, $\tau_n(t)$ is the time shifting and the ϕ_{D_n} is the Doppler effect. So the shortened form of the received signal is:

$$r(t) = \Re\left\{\sum_{n=0}^{N(t)} \alpha_n(t) e^{-j\phi_n(t)} u(t-\tau_n(t))] e^{j2\pi f_c t}\right\} \tag{4.5}$$

When we think of the channel as a linear time-varying system with a baseband channel impulse response $h(t,\tau)$, we may write $(t) = \Re\{\int_{-\infty}^{\infty} h(t,\tau)u(t-\tau)d\tau] e^{j2\pi f_c t}\}$, which is a straightforward expression.

When we compare this to (4.3), we get the following impulse response for a fading channel:

$$h(t,\tau) = \sum_{n=0}^{N(t)} \alpha_n(t) e^{-j\phi_n(t)} \delta(\tau - \tau_n(t)) \tag{4.6}$$

where $\delta(\cdot)$ is the dirac delta function. With this concept, we produced our wireless channel.

4.2.2 Channel Estimation

The message signal is often corrupted as a result of the characteristics of the channel. Therefore, to recover the transmitted bits, it is necessary to estimate and correct the channel distortions in the receiver [72,73]. A preamble or pilot symbols that are known to both the transmitter and the receiver are used to estimate the channel response of the frequency components between the pilot tones. Different interpolation methods are also used to estimate the channel response of the frequency components between the pilot tones. In general, channel estimation may be performed using either the data signal or the training signal, or even both at the same time. Many various implementation characteristics, such as the needed performance, computational complexity, and time-variation of the channel, must be taken into account while selecting a channel estimating approach for the communication system. Pilot structures are classified into three categories based on how they are organized: block type, comb type, and lattice type [64-71].

A block-type pilot configuration is shown in Figure 4.6. For channel estimation purposes, pilot symbols are sent out on a periodic basis. To estimate the channel length along the time axis, we do a time-domain interpolation using this set of pilot data.

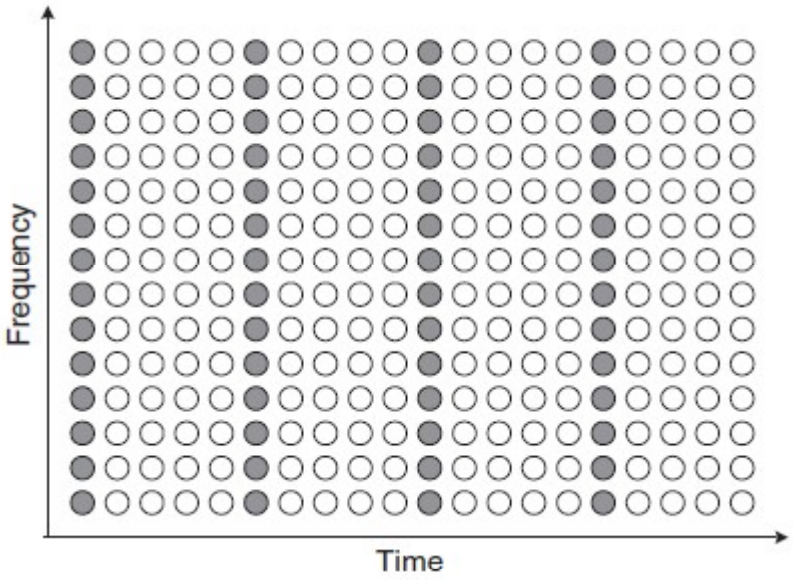

Figure 4.6 Block-type pilot arrangement. [64]

Due to the fact that pilot tones are introduced into all subcarriers of pilot symbols with a period in time, the block-type pilot arrangement is suited for frequency-selective transmission channels. In the case of fast-fading channels, however, it may be necessary to reduce the pilot symbol duration in order to avoid incurring extra costs in tracking the channel change.

Figure 4.7 depicts a pilot-type in the comb-type configuration. Pilot tones at the periodically placed subcarriers are employed in this sort of interpolation to estimate the channel along the frequency axis, which is done via frequency-domain interpolation. It is necessary to put pilot symbols on the channel as often as the coherent bandwidth in order to maintain track of the frequency-selective channel features. Contrary to the block-type pilot configuration, the comb-type pilot arrangement is ideal for fast-fading channels but not for frequency-selective channels.

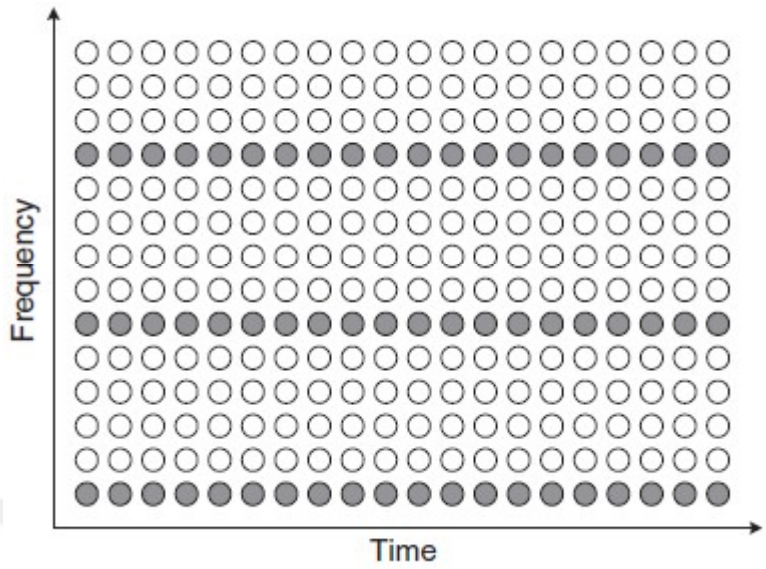

Figure 4.7 Comb-type pilot arrangement. [64]

Illustration of a lattice-type pilot configuration is shown in Figure 4.8. Pilot tones are introduced at specified periods along both the time and frequency axes in this sort of system. The pilot tones, which are spread over both the time and frequency axes, make it possible to perform time/frequency-domain interpolation for channel estimation purposes.

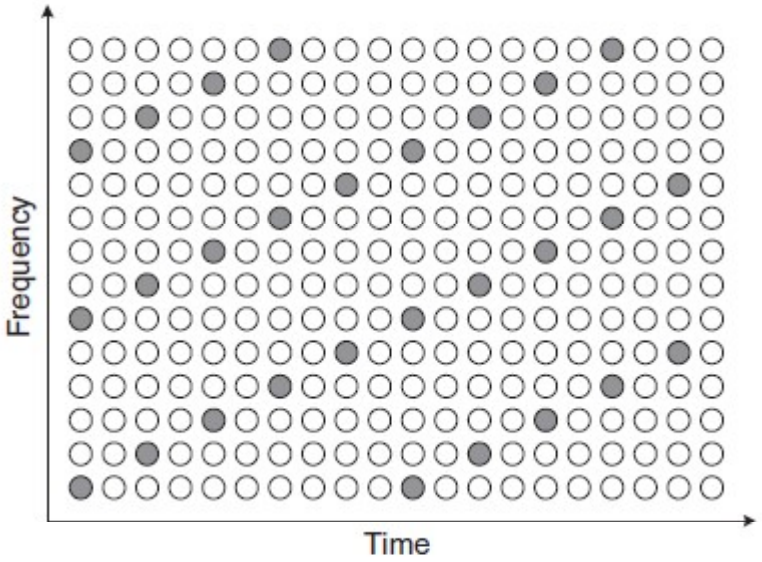

Figure 4.8 Lattice-type pilot arrangement [64]

For channel estimation, training symbols may be utilized, and the results are typically satisfactory. Unfortunately, their communication rates are diminished as a result of the additional overhead necessary to send training symbols such as preambles and pilot tones in addition to data symbols. As a result, when training symbols are available, the least-squares (LS) and minimum-mean-square-error (MMSE) approaches are often utilized for channel estimation [42,43].

4.2.3 Least Square Channel Estimation

It is possible to determine the channel $\widehat{H}$ using the least-square (LS) channel estimating technique in such a manner that the cost function (4.7) is minimized.

$$\begin{aligned} J(\widehat{H}) &= \left\| Y - X\widehat{H} \right\|^2 \\ &= \left(Y - X\widehat{H}\right)^H \left(Y - X\widehat{H}\right) \\ &= Y^H Y - Y^H X\widehat{H} - \widehat{H}^H X^H Y + \widehat{H}^H X^H X\widehat{H} \end{aligned} \tag{4.7}$$

By reducing the derivative of a function with reference to $\widehat{H}$ to zero, we may simplify the equation.

$$\frac{\partial J(\widehat{H})}{\partial \widehat{H}} = -2(X^H Y)^* + 2\left(X^H X\widehat{H}\right)^* = 0 \tag{4.8}$$

we have $X^H X\widehat{H} = X^H Y$. The answer to LS channel estimation is given by the following:

$$\widehat{H}_{LS} = (X^H X)^{-1} X^H Y = X^{-1} Y \tag{4.9}$$

Let us identify each component of the LS channel estimate with a different letter $\widehat{H}_{LS}$ by $\widehat{H}_{LS}[k], k = 0,1,2,\dots,N-1$. In light of the fact that X is expected to be diagonal owing to the ICI-free requirement, it is possible to write the LS channel estimate $\widehat{H}_{LS}$ for each subcarrier as

$$\widehat{H}_{LS}[k] = \frac{Y[k]}{X[k]}, k = 0,1,2, \dots, N-1 \tag{4.10}$$

The mean square error (MSE) of this LS channel estimation is provided as

$$\begin{aligned} MSE_{LS} &= E\left\{\left(H - \widehat{H}_{LS}\right)^H (H - H_{LS})\right\} \\ &= E\{(H - X^{-1}Y)^H (H - X^{-1}Y)\} \\ &= E\{(X^{-1}Z)^H (X^{-1}Z)\} \\ &= E\{Z^H (XX^H)^{-1} Z\} \\ &= \frac{\sigma_z^2}{\sigma_x^2} \end{aligned} \tag{4.11}$$

Consider that the MSE in Equation (4.11) is inversely proportional to the signal-to-noise ratio σ_x^2/σ_z^2. However, because of its simplicity, the LS approach has been frequently employed for channel estimate

4.2.4 MMSE Channel Estimation

In Equation (4.9), take into consideration the LS solution,$\widehat{H}_{LS} = X^{-1}Y \triangleq \widetilde{H}$. The weight matrix W is used to derive the value of $\widehat{H} \triangleq W\widetilde{H}$ which is equal to the MMSE estimate. According to Figure 4.9, the mean squared error of the channel estimate $\widehat{H}$ is given as

$$J(\widehat{H}) = E\{\|e\|^2\} = E\{\left\|H - \widehat{H}\right\|^2\} \tag{4.12}$$

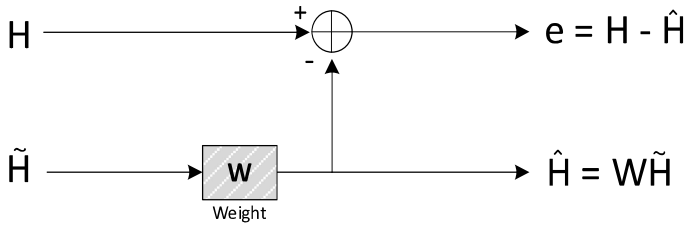

Figure 4.9 MMSE channel estimation

The MMSE channel estimation technique then finds a better (linear) estimate in terms of W in such a manner that the MSE in Equation (4.13) is reduced to the smallest possible value. Specifically, the orthogonality principle specifies that the estimate error vector $e = H - \widehat{H}$ is orthogonal to $\widetilde{H}$, such that

$$
\begin{aligned}
&E\{\widetilde{eH}^H\} = E\{(H - \widehat{H})\widetilde{H}^H\} \\
&= E\{(H - W\widetilde{H})\widetilde{H}^H\} \\
&= E\{H\widetilde{H}^H\} - WE\{\widetilde{H}\widetilde{H}^H\} \\
&= R_{H\widetilde{H}} - WR_{\widetilde{H}\widetilde{H}} = 0
\end{aligned} \tag{4.13}
$$

where R_{AB} is the cross-correlation matrix of NxN matrices A and B (i.e., $R_{AB} = E[AB^H]$), and $\widetilde{H}$ is the LS channel estimate given as

$$\widetilde{H} = X^{-1}Y = H + X^{-1}Z \tag{4.14}$$

Solving Equation (2.5) for W yields

$$W = R_{H\widetilde{H}}{R_{\widetilde{H}\widetilde{H}}}^{-1} \tag{4.15}$$

where $R_{\widetilde{H}\widetilde{H}}$ is the autocorrelation matrix of $\widetilde{H}$ given as;

$$
\begin{aligned}
&R_{\widetilde{H}\widetilde{H}} = E\{\widetilde{H}\widetilde{H}^H\} \\
&= E\{X^{-1}Y(X^{-1}Y)^H\} \\
&= E\{(H + X^{-1}Z)(H + X^{-1}Z)^H\} \\
&= E\{HH^H + X^{-1}ZH^H + HZ^H(X^{-1})^H + X^{-1}ZZ^H(X^{-1})^H)\}\} \\
&= E\{HH^H\} + E\{X^{-1}ZZ^H(X^{-1})^H) \\
&= E\{HH^H\} + \frac{\sigma_z^2}{\sigma_x^2}I
\end{aligned} \tag{4.16}
$$

and the cross-correlation matrix between the actual channel vector and the transient channel estimate vector in the frequency domain is denoted by the symbol $R_{\widetilde{H}\widetilde{H}}$.

The MMSE channel estimate is obtained by using Equation (4.16), which is written as

$$\widehat{H} = W\widetilde{H} = R_{H\widetilde{H}}{R_{\widetilde{H}\widetilde{H}}}^{-1}\widetilde{H} \tag{4.17}$$

$$= R_{H\tilde{H}}(R_{HH} + \frac{\sigma_z^2}{\sigma_x^2} I)^{-1} \tilde{H}$$

Specifically, the suggested structure makes use of a Frequency Domain Equalizer (FDE). It is no longer necessary to use an adaptive filter since the process of frequency-axis equalization is carried out by the equalizers themselves. In order to analytically explain this condition, as seen in Figure 4.10.

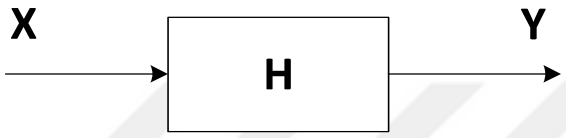

Figure 4.10: Frequency Domain Estimation

Our incoming signal to the frequency axis is equal to the product of our transmitted signal and the frequency response of our channel. To find the frequency response of the channel

$$H = Y/X \tag{4.18}$$

As show in Equation (4.18), it is sufficient to divide our incoming signal by our sent signal. As shown in Equation (4.19), if we multiply the inverse of the frequency response we get with our incoming signal, we get our sent X signal. This type of frequency domain equalizer is called Zero Forcing equalizer.

$$\begin{aligned} C &= H^{-1} \\ \hat{X} &= Y \times C \end{aligned} \tag{4.19}$$

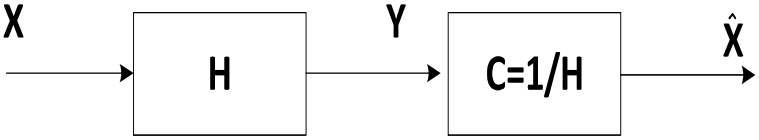

Figure 4.11: Frequency Domain Channel Equalizer

However, in cases where the effect of noise cannot be neglected, the Zero Forcing equalizer gives a loss. MMSE, on the other hand, considers the signal-to-noise ratio of the channel and determines an optimum value between the channel's response and the noise. It is expressed by Equation (4.20).

$$C = \frac{H^*}{|H| + (E_b/N_o)^{-1}} \tag{4.20}$$

The IFFT is then taken to retrieve our incoming signal in the time domain. In this method, we may acquire the actual signal in time domain that is free of the effects of the channel distortions.

4.3 CHANNEL ESTIMATED POLAR CODING OVER FADING CHANNEL RESULTS

In this section we implement LS and MMSE channel estimated polar coding over AWGN and Fading channels. The Rayleigh fading channel model is used. The flat fading channel model, where the fading is not very variable momentarily, was used in the test results. LS and MMSE figures were used as channel estimation methods. In addition, Zero Forcing based channel equalizer is preferred for channel equalization.

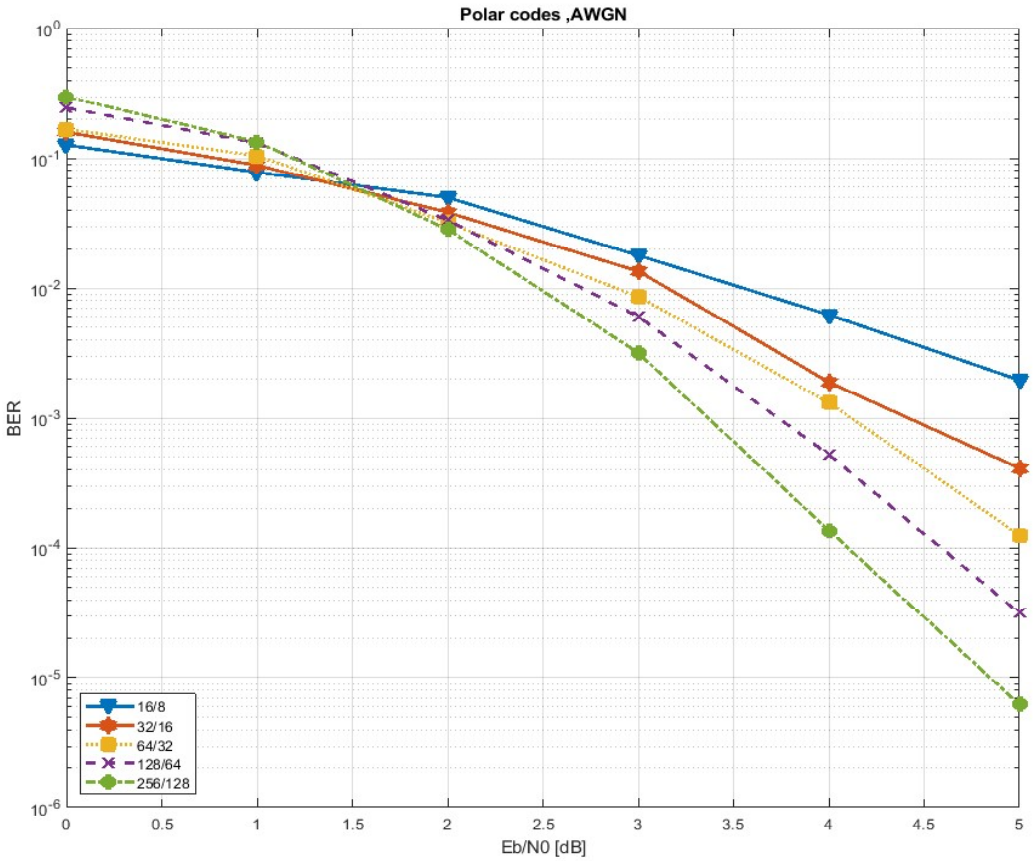

Figure 4.12 Bit error rate for polar code over AWGN Channel

The bit-error-rate (BER) performance of the polar code under the AWGN channel is depicted in Figure 4.12. Simulations are performed using BPSK modulation for AWGN channels. Polar codes with various codeword lengths $N = 16, 32, 64, 128$, and data lengths $K = 8, 16, 32, 64$ and with $rate = 1/2$ over the Rayleigh fading channel are tested.

Random data sequences were produced and used as the inputs of the system, after which the input sequences were encoded using a polar encoder to create the final output sequence. For frozen bits, ones are used. The polar coded data was modulated using a binary phase-shift keying (BPSK) modulator to get the final signal. Specifically, the codeword created by the polar encoder was mapped by the BPSK modulator. The

Rayleigh fading channel was used to transmit the modulated signal. Before the BPSK demodulation, the channel estimation and equalization are performed. Then, at the receiver, the SC decoder decodes and extracts the transmitted data.

Simulations are performed to get the performance of the proposed channel estimated polar decoding for AWGN and Rayleigh fading channels. The proposed idea is used for $N = 16$, $N = 64$, $N = 256$ over fading channel with LS and MMSE algorithm. It is seen that polar coding with MMSE-based channel segmentation performs better than LS-based channel coding. In Figure 4.13, FER performance curves for AWGN channels are depicted.

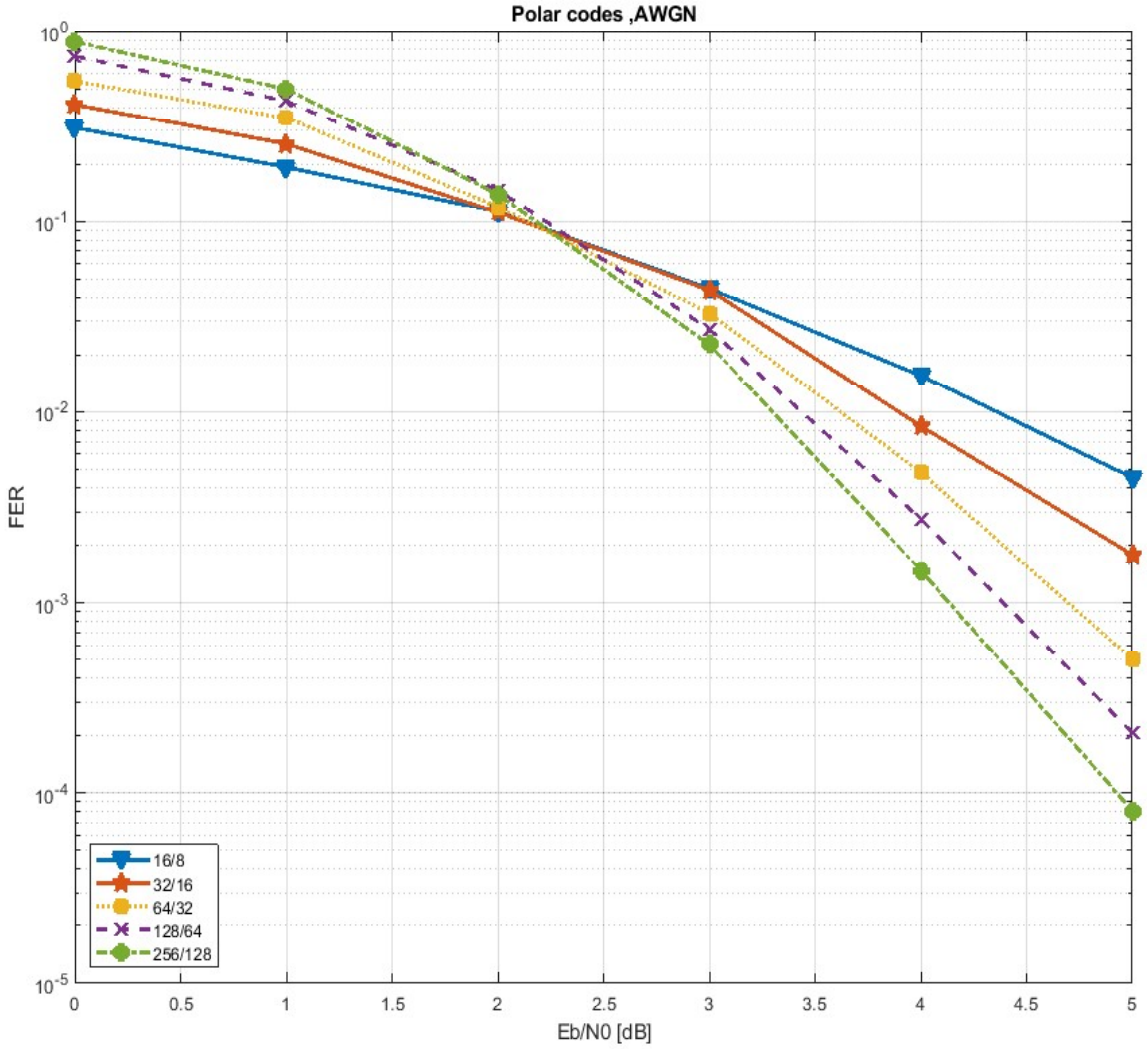

Figure 4.13 Frame error rate for polar code over AWGN Channel

MMSE estimated polar coded decoding outperforms the LS estimated decoding by 0.5 dB at $BER \cong 10^{-2}$ with BPSK modulation over fading channel, Figure 4.14. On the other hand, MMSE estimated polar coded decoding with higher block length outperforms the LS estimated decoding by $1dB$ at $BER \cong 10^{-2}$ over fading channel, Figure 4.15 and 4.16.

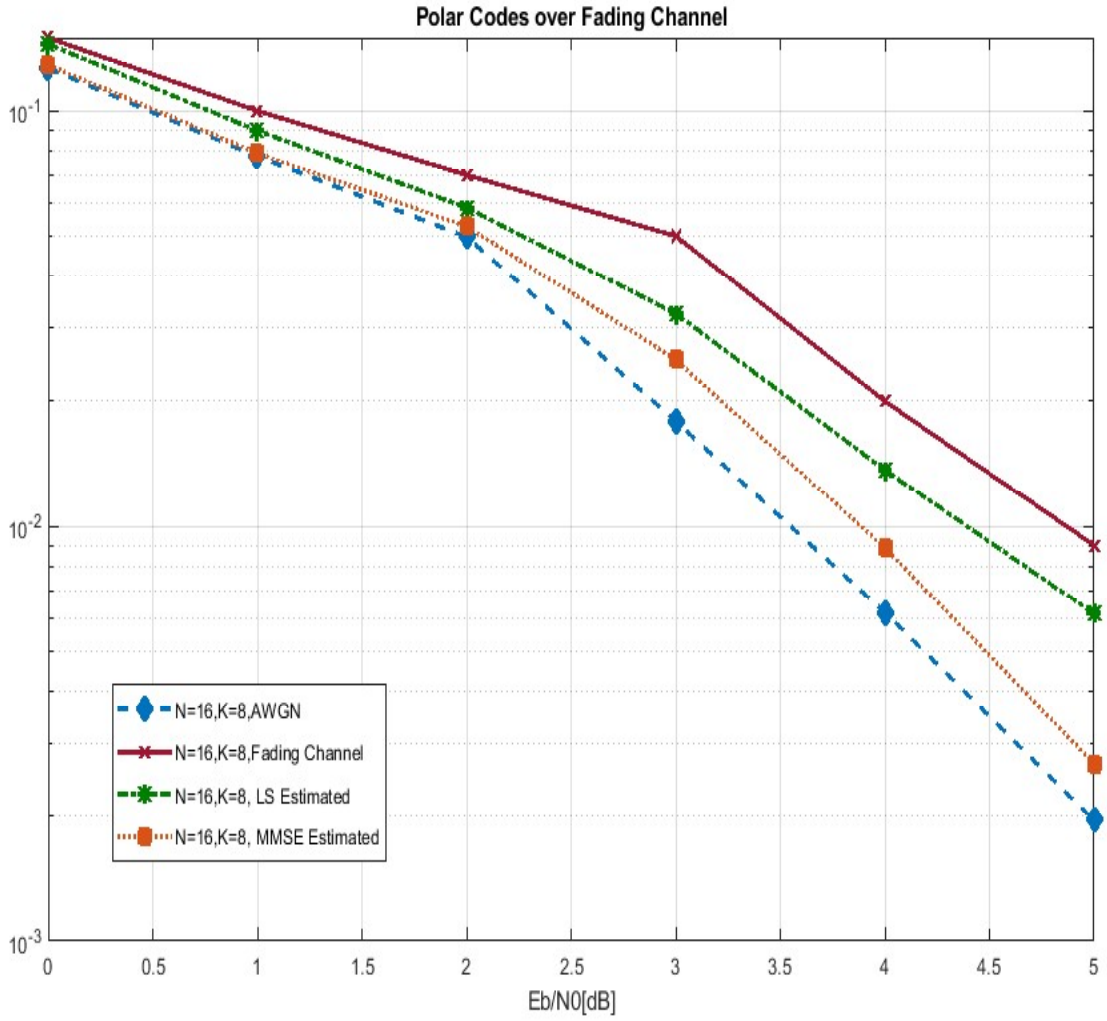

Figure 4.14 Bit error rate for polar code construction using our scheme over Rayleigh Fading Channel. The parameters of polar code are $N = 16, K = 8$.

BER performance in this situation converges to the same level as the BER performance in the AWG channel. This is because the MMSE algorithm is also based on the channel's SNR data. In this case, even if the fading effect of the channel is estimated with the frozen bits, the noise level can be determined as much as possible. Therefore, the BER performance of the MMSE algorithm converges to the BER performance of the AWGN channel.

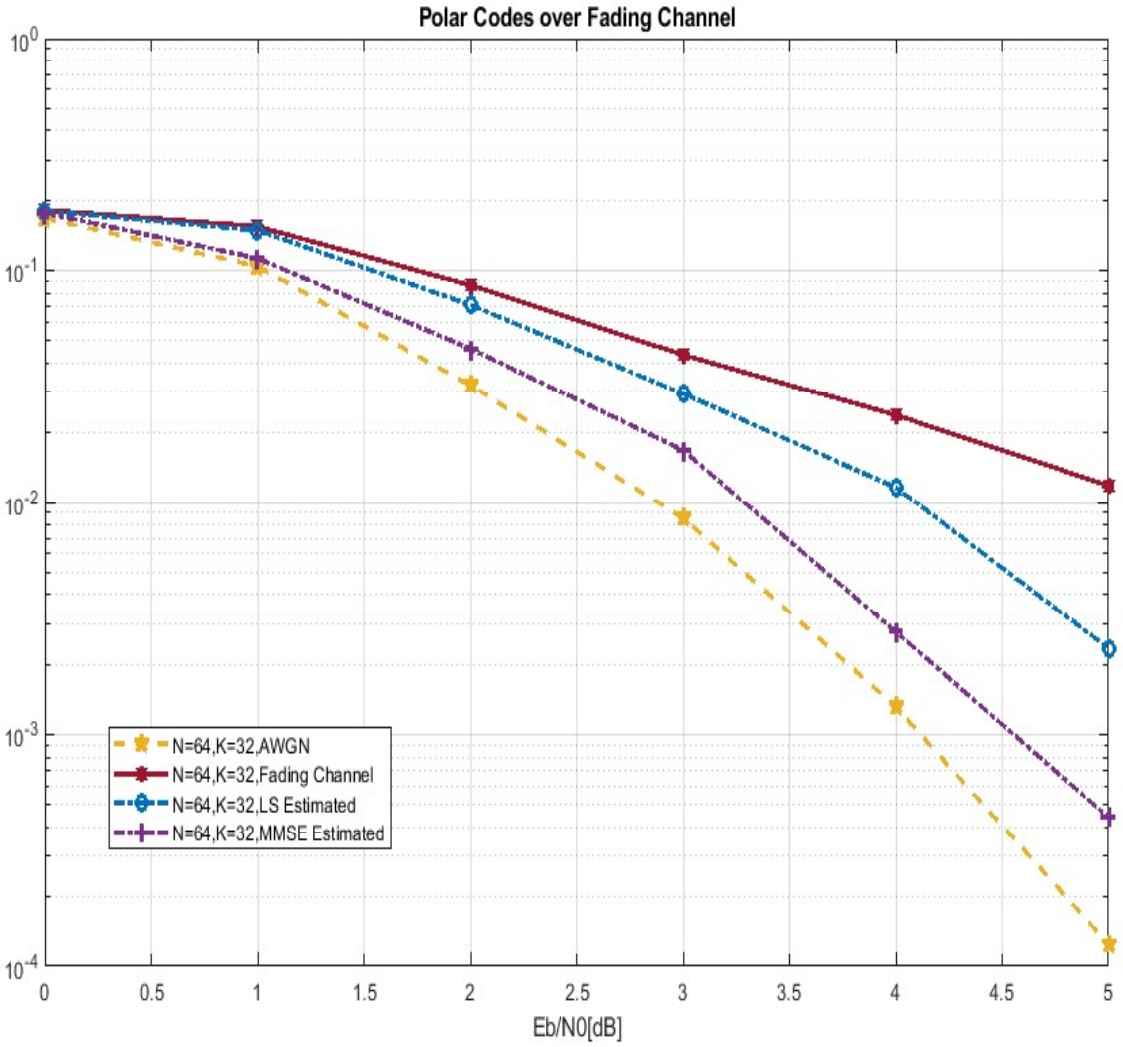

Figure 4.15 Bit error rate for polar code construction using our scheme over Rayleigh Fading Channel. The parameters of polar code are $N = 64, K = 32$.

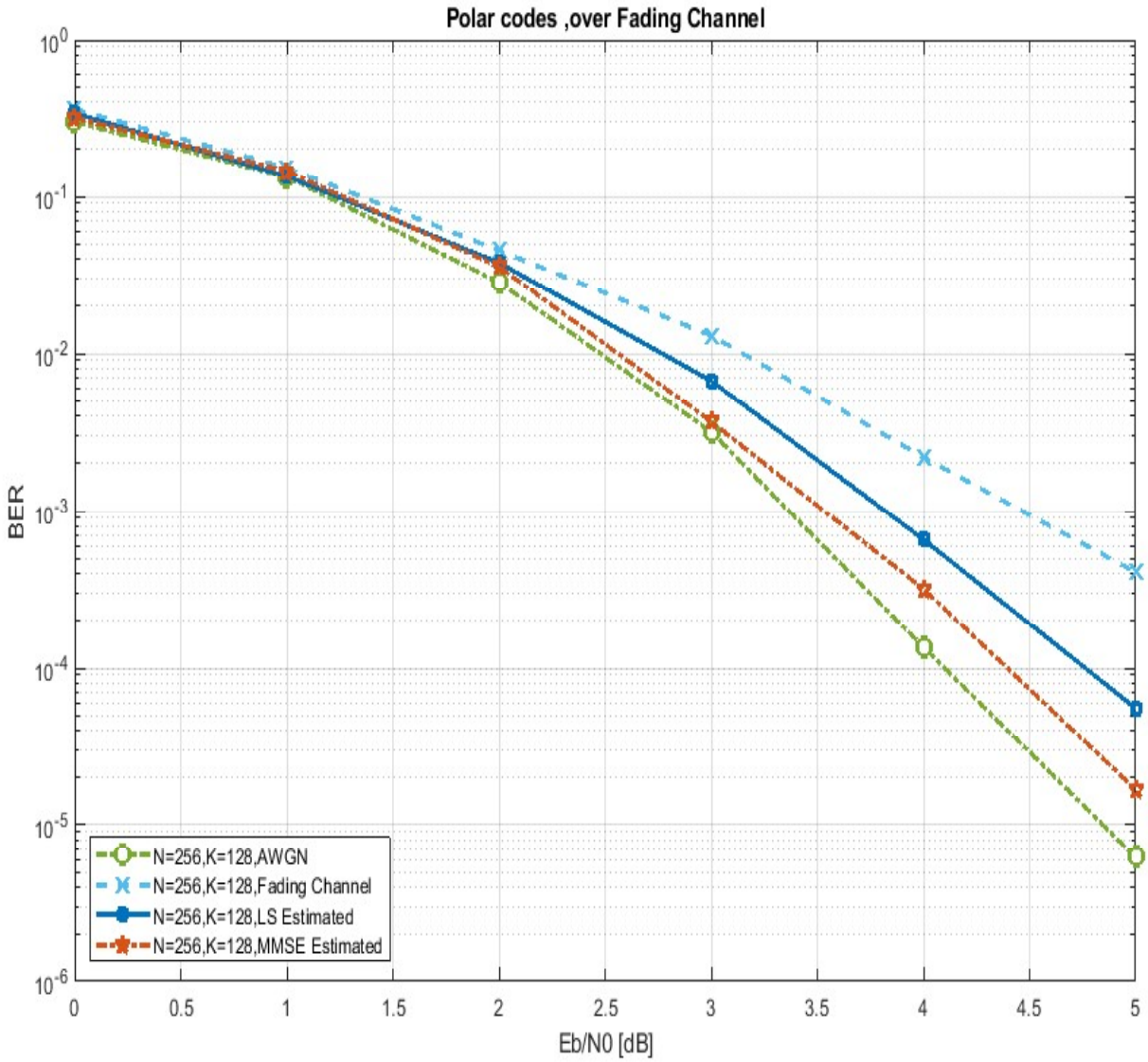

Figure 4.16 Bit error rate for polar code construction using our scheme over Rayleigh Fading Channel. The parameters of polar code are $N = 256, K = 128$.

CHAPTER V

CONCLUSION

In this thesis two independent topic related to the polar codes are investigated. The first one is implementation of polar encoding on a FPGA hardware. VHDL codes for the classical method were written and synthesized. Later, these codes were run on the Nexys3 FPGA board. Novel polar encoding method was proposed and the VHDL codes were written for the proposed encoding method. Concluded that the proposed scheme provides less space in a FPGA hardware and has less time-consuming property. Along with the conventional encoder technique, the suggested encoding approach helps reduce a huge proportion of the memory limitations that may be encountered during real application implementation. The results are relevant to practical cases in 5G wireless communication protocol.

Second topic we investigated in this thesis the employment of frozen bits for the channel estimation of fading channels. Frozen bit locations are calculated using Bhattacharyya parameter. The frozen bits are used for the channel estimation and equalization. The realization of channel estimation has been proven with the channel response information containing in the frozen bits. With the obtained channel response information, the channel equalization process was applied in the frequency domain. A great improvement in BER performance has been achieved with this method in fading channel. Besides, we compare the LS and MMSE based channel estimation method over the fading channel. The MMSE algorithm performs better than the LS algorithm. Unlike the LS algorithm, MMSE also quires the SNR information of the channel. For future work, a schema can be created where not all the frozen bits are used for channel estimation. A frozen pattern can be designed for different fading channels. It is anticipated that polar codes will continue to be a promising technique for the future communication standards.

REFERENCES

1. *"HF Band Frequency Hopping Physical Layer Algorithms for Military Communications"*, ASELSAN A.Ş. HBT-IA-2011-025, 2011-2012.
2. *"Novel Performance Increasing Algorithms for Underwater Communications and applications with FPGA"*. TÜBİTAK: Cost 113E589 Action. 2014-2016.
3. *"Digital Receiver with FPGA. Space and Defence Technologies (SDT)"*. Code: TÜBİTAK-1007-BSBK-2014-02. 2015-2016
4. *"Optical Based Wireless Communication (LI-FI) Development of In-Flight-Entertainment (IFE) Systems for Civil Aircrafts"*. ASELSAN A.Ş. 2020-2021
5. Fatih Genç, Orhan Gazi, *"Fast Calculation of Polar Code Bits and Frozen-Bit Locations"*. CUSJE 18(2):125-132 2021.e-ISSN:2564-7954.
6. Fatih Genç, Asuman Yavanoğlu, Anıl Reşat and Özgür Ertuğ. "*On the Comparative Performance Analysis of Turbo-Coded Non-Ideal Single-Carrier and Multi-Carrier Waveforms over Wideband Vogler-Hoffmeyer HF Channels*". Radioengineering Journal, Vol. 23, No. 3, pp. 872-879, September 2014.
7. Fatih Genç, Emre Yengel "*An Improved MMSE-Based Estimation Algorithm for Coherent Wireless UnderWater Optical OFDM Communication System*" Commun. Fac.Sci.Uni.Ank Series A2-A3, Volume 57, Number2, pages 25-38 (2015).
8. YILDIZ A.Ş., YARDIM F.E., AKÇAM N., GENÇ F., ", 2015. *LTE (4G)'nin Çoklu Anten Performans Analizleri,* 3trd International Symposium on Innovative Technologies in Engineering and Science (ISITES 2015), Pages:1668-1676, 18-20 June Valencia, Spain.
9. Fatih Genç, Mustafa Anıl Reşat, Asuman Savaşçıhabeş, Özgür Ertuğ. (2015) *"Performance modelling of turbo-coded non-ideal single-carrier and multi-carrier waveforms over wide-band Vogler-Hoffmeyer HF channels*." "Electronics,

Communications and Networks IV. Taylor & Francis Group, London, ISBN: 978-1-138-02830-2.

10. Aysan Keskin, Ömer Kemal Çakmataş, Fatih Genç, Serap Altay Arpalı, Yahya Baykal Çağlar Arpalı, "*Comparison of Effect of Collimated and Focused Laser Beam in Underwater Wireless Optical Communication."* IWOW 2015 Conference.
11. F. Genç, Mustafa Anıl Reşat, Asuman Savaşçıhabeş, Özgür Ertuğ. "*Tekli Taşıyıcılı ve Çoklu Taşıyıcılı Dalga Biçimlerin İdeal Olmayan Geniş Bant HF Kanallarda Karşılaştırılması.*" URSI-Türkiye' 2014 VII. Bilimsel Kongresi, 28-29 Ağustos 2014.
12. Fatih Genç, Asuman Yavanoğlu, Anıl Reşat and Özgür Ertuğ. "*Performance modelling of turbo-coded non-ideal single-carrier and multi-carrier waveforms over wide-band Vogler-Hoffmeyer HF channels".* Electronics, Communications and Networks IV. 2015 Taylor & Francis Group, London, ISBN: 978-1-138-02830-2.
13. Fatih Genç, Emre Yengel, Asuman Yavanoğlu, Özgür Ertuğ *"OFDM Sistemlerde 16-DAPSK Modülasyonunda Optimum Halka Oranın Belirlenmesi"* Signal Processing and Communications Application Conference, 22nd, 2014.
14. Shannon, C. E., (1948b), "*A mathematical Theory of Communication*", Bell Syst. Tech. J., vol. 27, pp. 623-656. October.
15. Arıkan E., (2009), "*Channel polarization: A method for constructing capacity-achieving codes for symmetric binary-input memoryless channels*", IEEE Trans. Inf. Theory, vol. 55, pp. 3051 – 3073.
16. 3GPP, (2018), "*Multiplexing and channel coding (Release 10) 3GPP TS 21.101 v10.4.0*", Oct. 2018.
17. Hussami N., Korada S. B. and Urbanke R., (2009), "*Performance of polar codes for channel and source codin*g", 2009 IEEE International Symposium on Information Theory, Seoul, pp. 1488-1492.
18. Çaycı S., (2013), "*Lossless data compression with polar codes*", A Thesis Submitted to The Graduate School of Engineering and Science of Bilkent University, 62 pages.
19. Önay S., (2014), "*Polar codes for distributed source coding*", A Thesis Submitted to The Graduate School of Engineering and Science of Bilkent University, 170 pages.
20. Arıkan E., (2010), "*Polar codes: A pipelined implementation*", 4th Int. Symp. Broadband Commun. (ISBC 2010), pp. 2–4.

21. Goela N., Korada S. B., and Gastpar M., (2010), "*On LP decoding of polar codes*", in 2010 IEEE Information Theory Workshop, ITW 2010 - Proceedings.
22. Poyraz E., Kim H., and Markarian G., (2009), "*Performance of short polar codes under ML decoding*", in ICT-Mobile Summit 2009 Conference Proceedings. pp 1-6.
23. Tal, I., & Vardy, A. (2013). "How to construct polar codes." IEEE Transactions on Information Theory, *59*(10), 6562–6582, doi: 10.1109/TIT.2013.2272694
24. I. Tal and A. Vardy, (2015), "*List Decoding of Polar Codes*", IEEE Trans. Inf. Theory, vol. 61, no. 5, pp. 2213–2226.
25. C. Leroux, I. Tal, A Vardy, and W. J. Gross, "Hardware architectures for successive cancellation decoding of polar codes," in IEEE Int. Con] Acoustics, Speech and Sig. Process. (ICASSP 2011), May 2011, pp. 1665-1668.
26. A Pamuk, "An FPGA implementation architecture for decoding of polarcodes," in Proc. 8th Symp. Wireless Commun. Syst. (ISWCS), Nov. 2011, pp. 437-441.
27. Mamatha. Sarah. Oommen, S. Ravishankar, "FPGA Implementation of an Advanced Encoding and Decoding Architecture of Polar Codes", 2015 International Conference on VLSI Systems, Architecture, Technology (VLSI-SATA).
28. Manohar Ayinala, Michael Brown, Keshab K.Parhi, "Pipelined Parallel FFT Architectures via Folding Transformation" IEEE Transactions On Very Large Scale Integration (Vlsi) Systems, Vol. 20, No. 6, June 2012.
29. Yoo, Hoyoung, and I. C. Park. "Partially Parallel Encoder Architecture for Long Polar Codes." IEEE Transactions on Circuits & Systems II Express Briefs 62.3(2015):306-310.
30. Raj, U. Mahendra Narasimha, and E. V. Narayana. "An advanced architecture with low complexity of partially parallel polar encoder." International Conference on Communication and Electronics Systems IEEE, 2017:1-5.
31. Arpure, Alok, and S. Gugulothu. "FPGA implementation of polar code-based encoder architecture." International Conference on Communication and Signal Processing IEEE, 2016:0691-0695.
32. 3GPP TSG RAN WG1 #87 Meeting MMC. Final Report of 3GPP TSG RAN WG1 #87 v1.0.0 [DB/OL]. [2017-6-30]. http://www.3gpp.org/ftp/tsg_ran/WG1_RL1/TSGR1_87/Report/

33. 3GPP TSG RAN WG1 #89 Meeting MMC. Final Report of 3GPP TSG RAN WG1 #88bis v1.0.0 [DB/OL]. [2017-6-30]. http://www.3gpp.org/ftp/tsg_ran/WG1_RL1/TSGR1_88b/Report/
34. Huawei, HiSilicon. Polar Coding Design for Control Channel [DB/OL]. [2017-6-30]. http://www.3gpp.org/ftp/tsg_ran/WG1_RL1/TSGR1_88b/Docs/
35. 3GPP TSG RAN WG1 #88 Meeting MMC. Final Report of 3GPP TSG RAN WG1 #88 v1.0.0 [DB/OL]. [2017-6-30]. http://www.3gpp.org/ftp/tsg_ran/WG1_RL1/TSGR1_88/Report/
36. Samsung. Maximum Polar Code Size [DB/OL]. [2017-6-30]. http://www.3gpp.org/ftp/tsg_ran/WG1_RL1/TSGR1_88/Docs/
37. Polaran. Polar Encoder [EB/OL], [2017-6-21]. http://polaran.com/documents/PB-PE-NE-1.0.pdf
38. Y. Li, R. Liu, and R. Wang, “A low-complexity SNR estimation algorithm based on frozen bits of polar codes,” IEEE Communications Letters, vol. 20, no. 12, pp. 2354–2357, 2016.
39. R. P. David and C. B. Norman, “A comparison of SNR estimation techniques for the AWGN channel,” IEEE Transactions on Communications, vol. 48, no. 10, pp. 1681–1691, 2000.
40. T. Salman, A. Badawy, T. M. Elfouly, and et al, “Non-data-aided snr estimation for QPSK modulation in AWGN channel,” in 2014 IEEE 10th International Conference on Wireless and Mobile Computing, Networking and Communications (WiMob), Larnaca, Cyprus, 2014, pp. 611–616.
41. N. Wu, H. Wang, and J. M. Kuang, “Code-aided SNR estimation based on expectation maximisation algorithm,” Electronics Letters, vol. 44, no. 15, pp. 924–925, 2008.
42. Z. Li, D. Yang, H. Wang, N. Wu, and J. Kuang, “Maximum likelihood SNR estimation for coded M-apsk signals in slow fading channels,” in 2013 International Conference on Wireless Communications and Signal Processing, Hangzhou, China, 2013.
43. A. Bravo-Santos, “Polar codes for the Rayleigh fading channel,” IEEE Communications Letters, vol. 17, no. 12, pp. 2352–2355, 2013.
44. S. R. Tavildar, “An interleaver design for polar codes over slow fading channels,” arXiv preprint arXiv:1610.04924, 2016.

45. J. J. Boutros and E. Biglieri, “Polarization of quasi-static fading channels,” in Information Theory Proceedings (ISIT), 2013 IEEE International Symposium on. IEEE, 2013, pp. 769–773.
46. D. R. Wasserman, A. U. Ahmed, and D. W. Chi, “BER performance of polar coded OFDM in multipath fading,” arXiv preprint arXiv:1610.00057, 2016.
47. H. Si, O. O. Koyluoglu, and S. Vishwanath, “Polar coding for fading channels: binary and exponential channel cases,” *IEEE Transactions on Communications, vol. 62, no. 8, pp. 2638–2650, 2014.*
48. L. Liu and C. Ling, “Polar codes and polar lattices for independent fading channels,” IEEE Transactions on Communications, vol. 64, no. 12, pp. 4923–4935, 2016.
49. M. Zheng, M. Tao, W. Chen, and C. Ling, “Polar coding for block fading channels,” arXiv preprint arXiv:1701.06111, 2017.
50. E. Abbe and E. Telatar, “Polar codes for the-user multiple access channel,” IEEE Transactions on Information Theory, vol. 58, no. 8, pp. 5437–5448, 2012.
51. Niu K. and Chen K., (2012), “*Stack decoding of polar codes*”, in Electronics Letters, vol. 48, no. 12, pp. 695 -697, June.
52. Vangala H., Viterbo E. and Hong Y., (2015), “*A Comparative Study of Polar Code Constructions for the AWGN Channel*”, arXiv:1501.02473 [cs.IT], Jan.
53. A. Bravo-Santos, *“Polar codes for the Rayleigh fading channel,”* IEEE Communications Letters, vol. 17, no. 12, pp. 2352–2355, 2013.
54. Liu, S., Hong, Y., & Viterbo, E. (2017). *“Polar Codes for Block Fading Channels.”* 2017 IEEE Wireless Communications and Networking Conference Workshops, WCNCW 2017, 1–6, doi: 10.1109/WCNCW.2017.7919041.
55. Trifonov P., (2012), “*Efficient Design and Decoding of Polar Codes*”, IEEE Trans. Commun., vol. 60, no. 11, pp. 3221–3227, Nov.
56. H. Vangala, E. Viterbo, and Y. Hong, *“A comparative study of polar code constructions for the AWGN channel,”* arXiv preprint arXiv:1501.02473, 2015.
57. D. R. Wasserman, A. U. Ahmed, and D. W. Chi, *“BER performance of polar coded OFDM in multipath fading,”* arXiv preprint arXiv:1610.00057, 2016.

58. Sutera A., (1980), *"Stochastic perturbation of a pure convective motion"*, Journal of the Atmospheric Sciences, vol. 37, pp. 245-249.
59. Di C., Proietti D., Telatar I. E., Richardson T. J. and Urbanke R. L., (2002), "*Finite-length analysis of low-density parity-check codes on the binary erasure channel*", IEEE Trans. Inf. Theory, vol. 48, no. 6, pp. 1570–1579.
60. Eslami A. and Pishro-Nik H., (2010), "*On bit error rate performance of polar codes in finite regime*", in 2010 48th Annual Allerton Conference on Communication, Control, and Computing (Allerton), pp. 188–194.
61. Orlitsky A., Urbanke R., Viswanathan K. and Zhang J., (2002), "*Stopping sets and the girth of Tanner graphs*", Proceedings IEEE International Symposium on Information Theory, Lausanne, pp. 2.
62. Xu M., Liang X., Zhang C., Wu Z., and You X., (2016), "*Stochastic BP Polar Decoding and Architecture with Efficient Re-Randomization and Directive Register*", in 2016 IEEE International Workshop on Signal Processing Systems (SiPS), pp. 315–320.
63. Han K., Wang J. and Gross W. J., (2018), "*Bit-Wise Iterative Decoding of Polar Codes using Stochastic Computing*", in Proceedings of the 2018 on Great Lakes Symposium on VLSI (GLSVLSI '18), pp. 409-414.
64. Coleri, S., Ergen, M., Puri, A., and Bahai, A. (2002). "*Channel estimation techniques based on pilot arrangement inOFDM systems." IEEE Trans. on Broadcasting, 48(3), 223–229.*
65. Heiskala, J. and Terry J. (2002). *"OFDM Wireless LANs: A Theoretical and Practical Guide", SAMS.*
66. Hsieh, M. and Wei, C. (1998). *"Channel estimation for OFDM systems based on comb-type pilot arrangement infrequency selective fading channels." IEEE Trans. Consumer Electron., 44(1), 217–228.*
67. Van Nee, R. and Prasad, R. (2000) "*OFDM for Wireless Multimedia Communications", Artech House Publishers.*
68. Lau, H.K. and Cheung, S.W. (May 1994) *"A pilot symbol-aided technique used for digital signals in multipath environments." IEEE ICC'94, vol. 2, pp. 1126–1130.*

69. Yang,W.Y., Cao,W., Chung, T.S., and Morris, J. (2005). *"Applied Numerical Methods Using MATLAB", JohnWiley & Sons, Inc., New York.*
70. Minn, H. and Bhargava, V.K. (1999) *"An investigation into time-domain approach for OFDM channel estimation.", IEEE Trans. on Broadcasting, 45(4), 400–409.*
71. Fernandez-Getino Garcia, M.J., Paez-Borrallo, J.M., and Zazo, S. (May 2001) *"DFT-based channel estimation in 2D-pilot-symbol-aided OFDM wireless systems." IEEE VTC'01, vol. 2, pp. 810–814.*
72. Tufvesson, F. and Maseng, T. (May 1997) *"Pilot assisted channel estimation forOFDMin mobile cellular systems." IEEE VTC'97, vol. 3, pp. 1639–1643.*
73. van de Beek, J.J., Edfors, O., Sandell, M. et al. (July 1995) *"On channel estimation in OFDM systems.", IEEE VTC'95, vol. 2, pp. 815–819.*
74. Li H. and Yuan J., (2013), "*A practical construction method for polar codes in AWGN channels*", IEEE 2013 Tencon - Spring, Sydney, NSW, pp. 223-226.
75. Ahmet Çağrı Arlı., (2020) "*Polar Code Decoding with Soft Decision Algorithms",* A Thesis Submitted to The Graduate School of Engineering and Science of Çankaya University, 129 pages.